

Model-independent Study of Magnetic Dipole Transitions in Quarkonium

Nora Brambilla, Yu Jia and Antonio Vairo¹

¹*Dipartimento di Fisica dell'Università di Milano and INFN,
via Celoria 16, 20133 Milano, Italy*

Abstract

We study magnetic dipole (M1) transitions between two quarkonia in the framework of non-relativistic effective field theories of QCD. Relativistic corrections of relative order v^2 are investigated in a systematic fashion. Non-perturbative corrections due to color-octet effects are considered for the first time and shown to vanish at leading order. Exact, all order expressions for the relevant $1/m$ and $1/m^2$ operators are derived. The results allow us to scrutinize several potential model claims. In particular, we show that QCD excludes either contributions to the anomalous magnetic moment of the quarkonium induced by low-energy fluctuations or contributions to the magnetic dipole operators of the type induced by a scalar potential. Finally, we apply our results to the transitions $J/\psi \rightarrow \eta_c \gamma$, $\Upsilon(1S) \rightarrow \eta_b \gamma$, $\Upsilon(2S) \rightarrow \eta_b(2S) \gamma$, $\Upsilon(2S) \rightarrow \eta_b \gamma$, $\eta_b(2S) \rightarrow \Upsilon(1S) \gamma$, $h_b(1P) \rightarrow \chi_{b0,1}(1P) \gamma$ and $\chi_{b2}(1P) \rightarrow h_b(1P) \gamma$ by assuming these quarkonium states in the weak-coupling regime. Our analysis shows that the $J/\psi \rightarrow \eta_c \gamma$ width is consistent with a weak-coupling treatment of the charmonium ground state, while such a treatment for the hindered transition $\Upsilon(2S) \rightarrow \eta_b \gamma$ appears difficult to accommodate within the CLEO III upper limit.

PACS numbers: 12.38.-t, 12.39.Hg, 13.25.Gv

I. INTRODUCTION

The non-relativistic nature appears to be an essential ingredient to understand the dynamics of heavy quarkonia. It has been established soon after the discovery of the J/ψ in 1974 by many subsequent phenomenological studies on numerous observables of the $c\bar{c}$ and $b\bar{b}$ bound states. Hence, heavy quarkonium is characterized by the interplay among the several supposedly well-separated scales typical of a non-relativistic system: the heavy quark mass m , the inverse of the typical size of the quarkonium $1/r \sim mv$ and the binding energy $E \sim mv^2$, where $v \ll 1$ is the velocity of the heavy quark inside the quarkonium. Nowadays the effective field theory (EFT) approach has become the paradigm to disentangle problems with a hierarchy of well-separated scales. Two effective field theories, non-relativistic QCD (NRQCD) [1, 2] and potential NRQCD (pNRQCD) [3, 4], have been developed in the last decade. Applications of these two EFTs have led to a plethora of new results for several observables in quarkonium physics (for a review see [5]).

Among the observables that haven't yet been considered in an EFT framework, are radiative transition widths. They have been studied so far almost entirely within phenomenological models [6, 7, 8, 9, 10, 11, 12, 13, 14, 15, 16, 17, 18, 19] (a sum rule analysis is provided in [20]). For a recent review we refer to Eichten's contribution in [21]. A textbook presentation can be found in [22]. Mostly, the models are based on a non-relativistic reduction of some relativistic interaction assumed on a phenomenological basis. Eventually, a potential model coupled to electromagnetism is recovered. In this work, we will describe radiative transitions in the language of EFTs. In particular, we will employ pNRQCD to study radiative transitions in a model independent fashion.

Two dominant single-photon-transition processes, namely electric dipole (E1) and magnetic dipole (M1) transitions, are of considerable interest. Since, for reasons that will become clear in the following, M1 transitions are theoretically much cleaner than E1 transitions, we will restrict ourselves to M1 transitions in this work.¹

The kinematics of a transition $H \rightarrow H'\gamma$ in the rest frame of H , where H and H' are two quarkonia, is described in Fig. 1. In the non-relativistic limit, the M1 transition width

¹ However, E1 transitions are the most copiously observed, because their rates are enhanced by $1/v^2$ with respect to the M1 case. We will report about E1 transitions elsewhere.

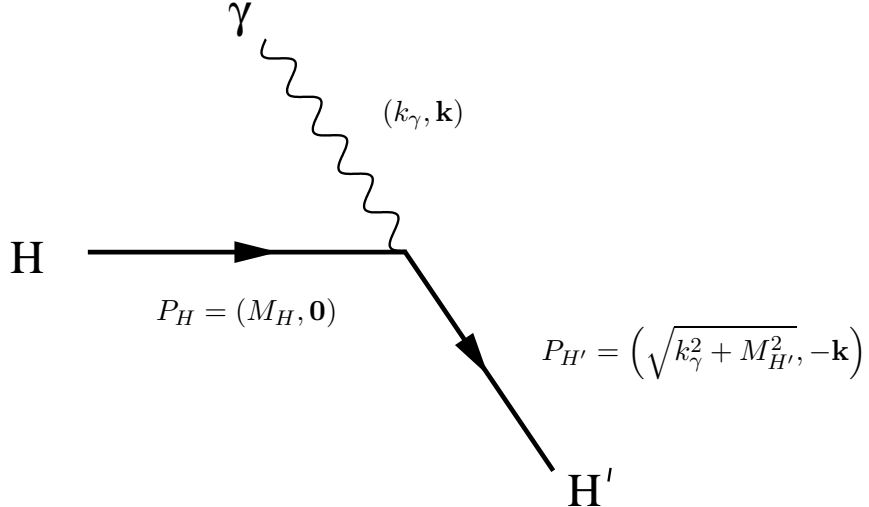


FIG. 1: Kinematics of the radiative transition $H \rightarrow H'\gamma$ in the rest frame of the initial-state quarkonium H . M_H and $M_{H'}$ are the masses of the initial and final quarkonium, and $k_\gamma = |\mathbf{k}| = (M_H^2 - M_{H'}^2)/(2M_H)$ is the energy of the emitted photon.

between two S -wave states is given by

$$\Gamma_{n^3S_1 \rightarrow n'{}^1S_0 \gamma} = \frac{4}{3} \alpha e_Q^2 \frac{k_\gamma^3}{m^2} \left| \int_0^\infty dr r^2 R_{n'0}(r) R_{n0}(r) j_0\left(\frac{k_\gamma r}{2}\right) \right|^2, \quad (1)$$

where ee_Q is the electrical charge of the heavy quark ($e_b = -1/3$, $e_c = 2/3$), α is the fine structure constant and $R_{nl}(r)$ are the radial Schrödinger wave functions. The photon energy k_γ is about the difference between the masses of the two quarkonia, therefore, it is of order mv^2 or smaller.² Since $r \sim 1/(mv)$, we may expand the spherical Bessel function $j_0(k_\gamma r/2) = 1 - (k_\gamma r)^2/24 + \dots$. At leading order in the multipole expansion, for $n = n'$, the overlap integral is 1. Such transitions are usually referred to as *allowed*. At leading order, for $n \neq n'$, the overlap integral is 0. These transitions are usually referred to as *hindered*. The widths of hindered transitions are entirely given by higher-order and relativistic corrections.

Equation (1) is not sufficient to explain the observed transition widths. In the case of allowed ones, for instance, it overpredicts the observed $J/\psi \rightarrow \eta_c \gamma$ transition rate by a factor 2 to 3. A large anomalous magnetic moment or large relativistic corrections have been advocated as a solution of this problem. Hence, it is crucial to supplement Eq. (1) with higher-order corrections. EFTs provide a systematic and controlled way for doing it.

² This is in sharp contrast with radiative transitions from a heavy quarkonium to a light meson, such as $J/\psi \rightarrow \eta\gamma$, whereas a hard photon is emitted.

EFTs are characterized by a power counting and a range of validity (the system must satisfy a hierarchy of scales). Errors are controlled by the power counting; higher-order corrections can be systematically included. Among these, EFTs include corrections coming from higher-Fock states, typically missed in potential models. In particular, in both NRQCD and pNRQCD color-octet contributions play a crucial role in some processes.

NRQCD is obtained from QCD by integrating out modes of energy m . The energy scale m is sometimes called *hard*. We denote with Λ_{QCD} the typical hadronic scale. Since $m \gg \Lambda_{\text{QCD}}$, the matching procedure that ensures the equivalence of the two theories may be carried out in perturbation theory. At this stage, also hard photons are integrated out. However, at the accuracy we are interested in, their contribution is negligible.

pNRQCD is obtained from NRQCD by integrating out modes of energy mv . This scale is sometimes called *soft*. We shall distinguish between *strongly coupled* quarkonia, for which $mv \sim \Lambda_{\text{QCD}}$ and *weakly coupled* quarkonia, for which $mv^2 \gtrsim \Lambda_{\text{QCD}}$. In the first case, the matching has to be done in a non-perturbative fashion. In the second case, it may be done order by order in the strong-coupling constant. Low-lying quarkonia are believed to be in the weak-coupling regime, higher excitations in the strong-coupling one. Soft photons are also integrated out at this stage, but give a contribution, which is numerically irrelevant with respect to that one coming from soft gluons. In the strong-coupling regime, the degrees of freedom of pNRQCD (coupled to electromagnetism) are singlet quarkonium fields and photons of energy and momentum of order mv^2 or smaller. The scale mv^2 is sometimes called *ultrasoft*. In the weak-coupling regime, there are also octet quarkonium fields and ultrasoft gluons. Ultrasoft fields are multipole expanded about the centre-of-mass coordinate. The power counting of the pNRQCD Lagrangian goes as follows. Ultrasoft gluons and virtual photons scale like mv^2 , the real photon, emitted in a single photon transition, like k_γ . In addition, the matching coefficients inherited from NRQCD are series in α_s . To simplify the counting, we will assume that $\alpha_s(m) \sim v^2$. In the weak-coupling regime, the matching coefficients of pNRQCD can be calculated in perturbation theory. Since the static potential is proportional to $\alpha_s(1/r)/r \sim mv^2$, it follows that $\alpha_s(1/r) \sim v$.

In the paper, we will mainly work out pNRQCD in the weak-coupling regime. Therefore, our final expressions will be applicable only to the lowest quarkonium resonances. However, some intermediate results will also apply to the strong-coupling regime. In particular, the $1/m$ and $1/m^2$ matching will be valid to all orders in α_s .

Some of the results presented here are new, some may be understood as a rewriting in the language of EFTs of results already derived long time ago in the framework of phenomenological models. Among others, we will address and answer the following questions. *(i)* What is the size of the quarkonium anomalous magnetic moment? *(ii)* Is there a scalar interaction contribution to M1 transitions? *(iii)* What is the size of the octet contributions to M1 transitions? We will end up with a rather concise formula which takes into account the full $\mathcal{O}(k_\gamma^3 v^2/m^2)$ relativistic corrections. We will clarify the validity and range of applicability of the widely-used formula of Ref. [15]. Applications to some M1 transitions between low-lying quarkonia will be discussed at the end.

The paper is organized as follows. In Sec. II, we first briefly review NRQCD and pNRQCD, then work out the basic formalism and calculate the transition widths in the non-relativistic limit. In Sec. III, we match the electromagnetic interaction Lagrangian of pNRQCD relevant for M1 transitions up to $1/m^3$ terms. In Sec. IV, we calculate contributions to the transition widths from wave-function corrections and, in particular, color-octet contributions. In Sec. V we sum all corrections and give the final formulae valid up to order $k_\gamma^3 v^2/m^2$. In Sec. VI, the decay rates of $J/\psi \rightarrow \eta_c \gamma$, $\Upsilon(1S) \rightarrow \eta_b \gamma$, $\Upsilon(2S) \rightarrow \eta_b(2S) \gamma$, $\Upsilon(2S) \rightarrow \eta_b \gamma$, $\eta_b(2S) \rightarrow \Upsilon(1S) \gamma$, $h_b(1P) \rightarrow \chi_{b0,1}(1P) \gamma$ and $\chi_{b2}(1P) \rightarrow h_b(1P) \gamma$ are calculated. Finally, in Sec VII we conclude. In one appendix, we discuss alternative ways to derive final-state recoil effects, in the other one, issues about gauge invariance.

II. MAGNETIC DIPOLE TRANSITIONS: BASIC FORMALISM

A. NRQCD

NRQCD is the EFT that follows from QCD by integrating out hard modes, i.e. modes of energy or momentum of order m [1, 2]. To describe electromagnetic transitions, we need to couple NRQCD to electromagnetism. For simplicity, we will call this new EFT also NRQCD. The effective Lagrangian is made of operators invariant under the $SU(3)_c \times U(1)_{\text{em}}$ gauge group. We display here only the part of the Lagrangian, which is relevant to describe M1

transitions at order $k_\gamma^3 v^2/m^2$:

$$\begin{aligned}
\mathcal{L}_{\text{NRQCD}} = & \psi^\dagger \left(iD_0 + \frac{\mathbf{D}^2}{2m} \right) \psi + \frac{c_F}{2m} \psi^\dagger \boldsymbol{\sigma} \cdot g \mathbf{B} \psi - \frac{c_s}{8m^2} \psi^\dagger \boldsymbol{\sigma} \cdot [-i\mathbf{D} \times, g\mathbf{E}] \psi \\
& + \frac{c_F^{\text{em}}}{2m} \psi^\dagger \boldsymbol{\sigma} \cdot ee_Q \mathbf{B}^{\text{em}} \psi - \frac{c_S^{\text{em}}}{8m^2} \psi^\dagger \boldsymbol{\sigma} \cdot [-i\mathbf{D} \times, ee_Q \mathbf{E}^{\text{em}}] \psi \\
& + \frac{c_{W1}^{\text{em}}}{8m^3} \psi^\dagger \{ \mathbf{D}^2, \boldsymbol{\sigma} \cdot ee_Q \mathbf{B}^{\text{em}} \} \psi - \frac{c_{W2}^{\text{em}}}{4m^3} \psi^\dagger \mathbf{D}^i \boldsymbol{\sigma} \cdot ee_Q \mathbf{B}^{\text{em}} \mathbf{D}^i \psi \\
& + \frac{c_{p'p}^{\text{em}}}{8m^3} \psi^\dagger (\boldsymbol{\sigma} \cdot \mathbf{D} ee_Q \mathbf{B}^{\text{em}} \cdot \mathbf{D} + \mathbf{D} \cdot ee_Q \mathbf{B}^{\text{em}} \boldsymbol{\sigma} \cdot \mathbf{D}) \psi \\
& + [\psi \rightarrow i\sigma^2 \chi^*] \\
& + \mathcal{L}_{\text{light}}, \tag{2}
\end{aligned}$$

where

$$\mathcal{L}_{\text{light}} = -\frac{1}{4} F^{\mu\nu a} F_{\mu\nu}^a - \frac{1}{4} F^{\mu\nu \text{em}} F_{\mu\nu \text{em}} + \sum_f \bar{q}_f i \not{D} q_f, \tag{3}$$

and ψ is the Pauli spinor field that annihilates a heavy quark of mass m , flavor Q and electrical charge ee_Q , χ is the corresponding one that creates a heavy antiquark, and q_f are the light quark Dirac fields. The gauge fields with superscript “em” are the electromagnetic fields, the others are gluon fields, $iD_0 = i\partial_0 - gT^a A_0^a - ee_Q A_0^{\text{em}}$, $i\mathbf{D} = i\boldsymbol{\nabla} + gT^a \mathbf{A}^a + ee_Q \mathbf{A}^{\text{em}}$, $[\mathbf{D} \times, \mathbf{E}] = \mathbf{D} \times \mathbf{E} - \mathbf{E} \times \mathbf{D}$, $\mathbf{E}^i = F^{i0}$, $\mathbf{B}^i = -\epsilon_{ijk} F^{jk}/2$, $\mathbf{E}^{i \text{em}} = F^{i0 \text{em}}$ and $\mathbf{B}^{i \text{em}} = -\epsilon_{ijk} F^{jk \text{em}}/2$ ($\epsilon_{123} = 1$).

The coefficients c_F , c_S , c_F^{em} , c_S^{em} , c_{W1}^{em} , c_{W2}^{em} and $c_{p'p}^{\text{em}}$ are the matching coefficients of the EFT. They satisfy some exact relations dictated by reparameterization (or Poincaré) invariance [23]:

$$c_S^{\text{em}} = 2c_F^{\text{em}} - 1, \quad c_S = 2c_F - 1, \tag{4}$$

$$c_{W2}^{\text{em}} = c_{W1}^{\text{em}} - 1, \tag{5}$$

$$c_{p'p}^{\text{em}} = c_F^{\text{em}} - 1. \tag{6}$$

Note that the $c_{W_i}^{\text{em}}$ are independent of c_F^{em} . All the coefficients are known at least at one loop [23]. In particular, we have

$$c_F^{\text{em}} \equiv 1 + \kappa_Q^{\text{em}} = 1 + C_F \frac{\alpha_s}{2\pi} + \mathcal{O}(\alpha_s^2), \tag{7}$$

$$c_{W1}^{\text{em}} = 1 + C_F \frac{\alpha_s}{\pi} \left(\frac{1}{12} + \frac{4}{3} \ln \frac{m}{\mu} \right) + \mathcal{O}(\alpha_s^2), \tag{8}$$

where $C_F = (N_c^2 - 1)/(2N_c) = 4/3$ and $C_A = N_c = 3$; κ_Q^{em} is usually identified with the anomalous magnetic moment of the heavy quark. Since c_{W1}^{em} and c_F^{em} are $\mathcal{O}(1)$, c_{W2}^{em} and $c_{p'p}^{\text{em}}$

are $\mathcal{O}(\alpha_s)$. κ_Q^{em} is less than 10% for charm and bottom. One may expect that the magnetic moment of the quarkonium may be larger than that, because, apart from inheriting the magnetic moments of the quarks, it may get potentially large low-energy contributions. We will clarify this point in Sec. III B.

In general, the matching coefficients will contain contributions coming from virtual photons of energy or momentum of order m , which have also been integrated out. These contributions are suppressed by order α and shall be neglected in the following. We will only consider QCD corrections.

B. pNRQCD

NRQCD still contains redundant degrees of freedom in describing a quarkonium state far below the open flavor threshold. pNRQCD is the EFT that follows from NRQCD by further integrating out quarks and gluons of momentum and energy of order mv and gluons of momentum of order mv and energy of order mv^2 [3, 4]. We consider here pNRQCD in the weak-coupling regime ($mv^2 \gtrsim \Lambda_{\text{QCD}}$). The degrees of freedom of pNRQCD are quarks of momentum mv and energy mv^2 and (ultrasoft) gluons of energy and momentum of order mv^2 . Since we are interested in quarkonium states, it is convenient to express the pNRQCD Lagrangian in terms of quark-antiquark fields. These are $3 \otimes 3$ tensors in color space and $2 \otimes 2$ tensors in spin space, which depend on the centre-of-mass coordinate \mathbf{R} and the relative distance \mathbf{r} of the two quarks. At leading order, the pNRQCD Lagrangian very much resembles a potential model, where the potentials are the matching coefficients of the EFT that encode the soft-scale contributions. The pNRQCD Lagrangian, however, also contains dynamical (ultrasoft) gluons and their interactions with the quark-antiquark fields.

Quarkonium radiative transitions involve real photons of energy and momentum k_γ of order mv^2 for hindered transitions and smaller for allowed ones. These transitions are described by pNRQCD if photons of momentum mv are integrated out from NRQCD and photons of energy and momentum of order mv^2 or lower are explicitly coupled to the quark fields in the pNRQCD Lagrangian. To ensure that gluons and photons are of energy and momentum not larger than mv^2 , all gauge fields are multipole expanded in the relative distance \mathbf{r} , and, therefore, depend on the centre-of-mass coordinate \mathbf{R} only.

Gauge invariance can be made manifest at the Lagrangian level by reexpressing the quark-

antiquark fields in terms of fields that transform like singlets under $U(1)_{\text{em}}$ and like singlets or octets under $SU(3)_c$ gauge transformations. We denote these fields as $S = S\mathbf{1}_c/\sqrt{N_c}$ and $O = \sqrt{2}O^aT^a$, respectively.

The pNRQCD Lagrangian, which is relevant to describe M1 transitions at order $k_\gamma^3 v^2/m^2$, is given by

$$\begin{aligned}
\mathcal{L}_{\text{pNRQCD}} = & \int d^3r \text{Tr} \left\{ S^\dagger \left(i\partial_0 + \frac{\nabla^2}{4m} + \frac{\nabla_r^2}{m} - V_S \right) S \right. \\
& + O^\dagger \left(iD_0 + \frac{\mathbf{D}^2}{4m} + \frac{\nabla_r^2}{m} - V_O \right) O \\
& + V_A (O^\dagger \mathbf{r} \cdot g\mathbf{E} S + S^\dagger \mathbf{r} \cdot g\mathbf{E} O) + V_B \frac{\{O^\dagger, \mathbf{r} \cdot g\mathbf{E}\}}{2} O \Big\} \\
& + \mathcal{L}_{\gamma \text{pNRQCD}} \\
& + \mathcal{L}_{\text{light}}, \tag{9}
\end{aligned}$$

where

$$\begin{aligned}
\mathcal{L}_{\gamma \text{pNRQCD}} = & \int d^3r \text{Tr} \left\{ V_A^{\text{em}} S^\dagger \mathbf{r} \cdot ee_Q \mathbf{E}^{\text{em}} S \right. \\
& + \frac{1}{2m} V_S^{\frac{\sigma \cdot B}{m}} \{S^\dagger, \boldsymbol{\sigma} \cdot ee_Q \mathbf{B}^{\text{em}}\} S \\
& + \frac{1}{16m} V_S^{(r \cdot \nabla)^2 \frac{\sigma \cdot B}{m}} \{S^\dagger, \mathbf{r}^i \mathbf{r}^j (\nabla^i \nabla^j \boldsymbol{\sigma} \cdot ee_Q \mathbf{B}^{\text{em}})\} S \\
& + \frac{1}{2m} V_O^{\frac{\sigma \cdot B}{m}} \{O^\dagger, \boldsymbol{\sigma} \cdot ee_Q \mathbf{B}^{\text{em}}\} O \\
& + \frac{1}{4m^2} \frac{V_S^{\frac{\sigma \cdot (r \times r \times B)}{m^2}}}{r} \{S^\dagger, \boldsymbol{\sigma} \cdot [\hat{\mathbf{r}} \times (\hat{\mathbf{r}} \times ee_Q \mathbf{B}^{\text{em}})]\} S \\
& + \frac{1}{4m^2} \frac{V_S^{\frac{\sigma \cdot B}{m^2}}}{r} \{S^\dagger, \boldsymbol{\sigma} \cdot ee_Q \mathbf{B}^{\text{em}}\} S \\
& - \frac{1}{16m^2} V_S^{\frac{\sigma \cdot \nabla \times E}{m^2}} [S^\dagger, \boldsymbol{\sigma} \cdot [-i\mathbf{\nabla} \times, ee_Q \mathbf{E}^{\text{em}}]] S \\
& - \frac{1}{16m^2} V_S^{\frac{\sigma \cdot \nabla_r \times r \cdot \nabla E}{m^2}} [S^\dagger, \boldsymbol{\sigma} \cdot [-i\mathbf{\nabla}_r \times, \mathbf{r}^i (\nabla^i ee_Q \mathbf{E}^{\text{em}})]] S \\
& + \frac{1}{4m^3} V_S^{\frac{\nabla_r^2 \sigma \cdot B}{m^3}} \{S^\dagger, \boldsymbol{\sigma} \cdot ee_Q \mathbf{B}^{\text{em}}\} \nabla_r^2 S \\
& \left. + \frac{1}{4m^3} V_S^{\frac{(\nabla_r \cdot \sigma) (\nabla_r \cdot B)}{m^3}} \{S^\dagger, \boldsymbol{\sigma}^i ee_Q \mathbf{B}^{\text{em}j}\} \nabla_r^i \nabla_r^j S \right\}. \tag{10}
\end{aligned}$$

If not differently specified, all gauge fields are calculated in the centre-of-mass coordinate \mathbf{R} , $iD_0 O = i\partial_0 O - g[T^a A_0^a, O]$, $i\mathbf{D}O = i\mathbf{\nabla}O + g[T^a \mathbf{A}^a, O]$, $\nabla^i = \partial/\partial \mathbf{R}^i$ and $\nabla_r^i = \partial/\partial \mathbf{r}^i$. The trace is over color and spin indices.

In the initial quarkonium rest frame, the power counting goes as follows:³ $\nabla_r \sim mv$, $r \sim 1/mv$ and $\mathbf{E}, \mathbf{B} \sim m^2v^4$. The electromagnetic fields associated to the external photon scale like $\mathbf{E}^{\text{em}}, \mathbf{B}^{\text{em}} \sim k_\gamma^2$. The centre-of-mass derivative ∇ acting on the recoiling final quarkonium state or emitted photon is of order k_γ . Operators that have not been displayed are suppressed either in the power counting or in the matching coefficients.

The coefficients V in Eqs. (9) and (10) are the matching coefficients of pNRQCD. The matching coefficients of Eq. (9) have been calculated in the past years. We refer the reader to [5] and references therein. In the following, we will calculate the matching coefficients of Eq. (10). Here, we only note that since $mv \gg \Lambda_{\text{QCD}}$, they may be calculated in perturbation theory. V_S and V_O play the role of a singlet and octet potential. They may be arranged in powers of $1/m$. The static contribution is the Coulomb potential:

$$V_S^{(0)} = -C_F \frac{\alpha_{V_S}}{r}, \quad V_O^{(0)} = \frac{1}{2N_c} \frac{\alpha_{V_O}}{r}, \quad (11)$$

where, at leading order, $\alpha_{V_S} = \alpha_{V_O} = \alpha_s$. In a Coulombic system $\alpha_s(1/r) \sim v$.

Let us discuss the different terms appearing in Eqs. (9) and (10). The first three lines of Eq. (9) display the pNRQCD Lagrangian in the limit of zero coupling to the photons. The third line describes the coupling of the quarkonium fields to ultrasoft gluons at order \mathbf{r} in the multipole expansion. Higher-order terms are irrelevant for the present purposes. At tree level, the coefficients V_A and V_B are equal to 1. Equation (10) provides the part of the pNRQCD interaction Lagrangian with the electromagnetic field relevant for M1 transitions. The first line describes the coupling of the quarkonium singlet field to ultrasoft photons at order \mathbf{r} . This is the familiar E1 transition operator ($V_A^{\text{em}} = 1$ at tree level). As we will discuss in the following, if the recoiling of the final quarkonium is taken into account, this term contributes to M1 transitions. A similar term involving the coupling with the octet field is suppressed in the transition amplitude. From the second line on, we display spin-dependent operators coupled to ultrasoft photons. Lines two and three come from multipole expanding the magnetic dipole operator at $\mathcal{O}(r^0)$ and $\mathcal{O}(r^2)$ respectively. The order \mathbf{r} term does not contribute to M1 transitions. Line four represents the leading magnetic dipole operator for octet quarkonium fields.

³ For simplicity, we give the power counting in the case $mv^2 \sim \Lambda_{\text{QCD}}$ only.

C. Radiative transitions

The process $H \rightarrow H'\gamma$ is described in the rest frame of the initial quarkonium state H by the kinematics of Fig. 1. The transition width is given by:

$$\begin{aligned}\Gamma_{H \rightarrow H'\gamma} &= \int \frac{d^3 P'}{(2\pi)^3} \frac{d^3 k}{(2\pi)^3} \frac{1}{2k} (2\pi)^4 \delta^4(P_H - k - P') \\ &\quad \times \frac{1}{N_\lambda} \sum_{\lambda\lambda'\sigma} |\mathcal{A}[H(\mathbf{0}, \lambda) \rightarrow H'(\mathbf{P}', \lambda')\gamma(\mathbf{k}, \sigma)]|^2 \\ &= \frac{1}{8\pi^2} \left(1 - \frac{k_\gamma}{M_H}\right) \int_0^\infty dk k \int d\Omega(\hat{\mathbf{k}}) \delta(k - k_\gamma) \\ &\quad \times \frac{1}{N_\lambda} \sum_{\lambda\lambda'\sigma} |\mathcal{A}[H(\mathbf{0}, \lambda) \rightarrow H'(-\mathbf{k}, \lambda')\gamma(\mathbf{k}, \sigma)]|^2, \quad (12)\end{aligned}$$

where $P'^\mu = (\sqrt{\mathbf{P}'^2 + M_{H'}^2}, \mathbf{P}')$, $k^\mu = (|\mathbf{k}|, \mathbf{k})$ and

$$\begin{aligned}\mathcal{A}[H(\mathbf{0}, \lambda) \rightarrow H'(-\mathbf{k}, \lambda')\gamma(\mathbf{k}, \sigma)] (2\pi)^3 \delta^3(\mathbf{P}' + \mathbf{k}) \\ = -\langle H'(\mathbf{P}', \lambda')\gamma(\mathbf{k}, \sigma) | \int d^3 R \mathcal{L}_{\gamma \text{pNRQCD}} |H(\mathbf{0}, \lambda)\rangle. \quad (13)\end{aligned}$$

In Eq. (12), the initial state is averaged over the polarizations, whose number is N_λ .

The quarkonium state $|H(\mathbf{P}, \lambda)\rangle$ is an eigenstate of the pNRQCD Hamiltonian with the quantum numbers of the quarkonium H . It has the non-relativistic normalization:

$$\langle H(\mathbf{P}', \lambda') | H(\mathbf{P}, \lambda) \rangle = \delta_{\lambda\lambda'} (2\pi)^3 \delta^3(\mathbf{P} - \mathbf{P}'). \quad (14)$$

The photon state $|\gamma(\mathbf{k}, \sigma)\rangle$ is normalized in the usual Lorentz-invariant way:

$$\langle \gamma(\mathbf{k}, \sigma) | \gamma(\mathbf{k}', \sigma') \rangle = 2k \delta_{\sigma\sigma'} (2\pi)^3 \delta^3(\mathbf{k} - \mathbf{k}'). \quad (15)$$

D. Quarkonium states

According to the power counting, the leading-order pNRQCD Hamiltonian is given by

$$H_{\text{pNRQCD}}^{(0)} = \int d^3 R \int d^3 r \text{Tr} \left\{ \mathbf{S}^\dagger h_S^{(0)} \mathbf{S} + \mathbf{O}^\dagger h_O^{(0)} \mathbf{O} \right\} + H_{\text{light}}, \quad (16)$$

where

$$h_S^{(0)} = -\frac{\nabla_r^2}{m} + V_S^{(0)}, \quad h_O^{(0)} = -\frac{\nabla_r^2}{m} + V_O^{(0)}, \quad (17)$$

and H_{light} is the Hamiltonian that corresponds to $\mathcal{L}_{\text{light}}$. The spectrum of pNRQCD has been first studied in [4], to which we refer for discussions. We call $|H(\mathbf{P}, \lambda)\rangle^{(0)}$ the subset of eigenstates made by a quark-antiquark pair in a singlet representation:

$$|H(\mathbf{P}, \lambda)\rangle^{(0)} = \int d^3R \int d^3r e^{i\mathbf{P}\cdot\mathbf{R}} \text{Tr} \left\{ \Phi_{H(\lambda)}^{(0)}(\mathbf{r}) S^\dagger(\mathbf{r}, \mathbf{R}) |0\rangle \right\}, \quad (18)$$

where $|0\rangle$ is a state that belongs to the Fock subspace containing no heavy quarks but an arbitrary number of ultrasoft gluons, photons and light quarks. The state $|0\rangle$ is normalized in such a way that Eq. (14) is fulfilled. The function $\Phi_{H(\lambda)}^{(0)}(\mathbf{r}) = \langle 0 | S(\mathbf{r}, \mathbf{R}) | H(\mathbf{0}, \lambda) \rangle^{(0)}$ is an eigenstate of the spin and orbital angular momentum of the quarkonium and satisfies the Schrödinger equation

$$h_S^{(0)} \Phi_{H(\lambda)}^{(0)}(\mathbf{r}) = E_H^{(0)} \Phi_{H(\lambda)}^{(0)}(\mathbf{r}). \quad (19)$$

$E_H^{(0)}$ is the leading-order binding energy of the quarkonium H : $M_H = 2m + E_H^{(0)}$. For later use, we write $\Phi_{H(\lambda)}^{(0)}$ for $L = 0$ states,

$$\Phi_{n^3S_1(\lambda)}^{(0)}(\mathbf{r}) = \frac{1}{\sqrt{4\pi}} R_{n0}(r) \frac{\boldsymbol{\sigma} \cdot \mathbf{e}_{n^3S_1}(\lambda)}{\sqrt{2}}, \quad (20)$$

$$\Phi_{n^1S_0}^{(0)}(\mathbf{r}) = \frac{1}{\sqrt{4\pi}} R_{n0}(r) \frac{1}{\sqrt{2}}, \quad (21)$$

where $\mathbf{e}_{n^3S_1}(\lambda)$ is the polarization vector of the state n^3S_1 , normalized as $\mathbf{e}_{n^3S_1}^*(\lambda) \cdot \mathbf{e}_{n^3S_1}(\lambda') = \delta_{\lambda\lambda'}$, and for $L = 1$ states,

$$\Phi_{n^1P_1(\lambda)}^{(0)}(\mathbf{r}) = \sqrt{\frac{3}{4\pi}} R_{n1}(r) \frac{\mathbf{e}_{n^1P_1}(\lambda) \cdot \hat{\mathbf{r}}}{\sqrt{2}}, \quad (22)$$

$$\Phi_{n^3P_0}^{(0)}(\mathbf{r}) = \sqrt{\frac{1}{4\pi}} R_{n1}(r) \frac{\boldsymbol{\sigma} \cdot \hat{\mathbf{r}}}{\sqrt{2}}, \quad (23)$$

$$\Phi_{n^3P_1(\lambda)}^{(0)}(\mathbf{r}) = \sqrt{\frac{3}{8\pi}} R_{n1}(r) \frac{\boldsymbol{\sigma} \cdot (\hat{\mathbf{r}} \times \mathbf{e}_{n^3P_1}(\lambda))}{\sqrt{2}}, \quad (24)$$

$$\Phi_{n^3P_2(\lambda)}^{(0)}(\mathbf{r}) = \sqrt{\frac{3}{4\pi}} R_{n1}(r) \frac{\boldsymbol{\sigma}^i h_{n^3P_2}^{ij}(\lambda) \hat{\mathbf{r}}^j}{\sqrt{2}}, \quad (25)$$

where $\mathbf{e}_{n^1P_1}(\lambda)$ and $\mathbf{e}_{n^3P_1}(\lambda)$ are polarization vectors satisfying $\mathbf{e}_{n^1P_1}^*(\lambda) \cdot \mathbf{e}_{n^1P_1}(\lambda') = \mathbf{e}_{n^3P_1}^*(\lambda) \cdot \mathbf{e}_{n^3P_1}(\lambda') = \delta_{\lambda\lambda'}$, whereas the polarization of the n^3P_2 state is represented by a symmetric and traceless rank-2 tensor $h_{n^3P_2}^{ij}(\lambda)$ normalized according to $h_{n^3P_2}^{ij*}(\lambda) h_{n^3P_2}^{ji}(\lambda') = \delta_{\lambda\lambda'}$.

The state $|H(\mathbf{P}, \lambda)\rangle$ may be obtained from $|H(\mathbf{P}, \lambda)\rangle^{(0)}$ by quantum-mechanical perturbation theory. At relative order v^2 the following corrections may be relevant.

1. Higher-order potentials

In the weak-coupling regime, corrections to the zeroth-order pNRQCD Hamiltonian of the type

$$\delta H = \int d^3R \int d^3r \text{Tr} \{ S^\dagger \delta V_S S \} ,$$

are typically suppressed by v^2 with respect to the leading term. First-order corrections to the quarkonium state, induced by these terms, are therefore relevant at relative order v^2 :

$$|H(\mathbf{P}, \lambda)\rangle^{(1)} = \int d^3R \int d^3r e^{i\mathbf{P}\cdot\mathbf{R}} \text{Tr} \{ \delta\Phi_{H(\lambda)}(\mathbf{r}) S^\dagger(\mathbf{r}, \mathbf{R}) |0\rangle \} , \quad (26)$$

where

$$\delta\Phi_{H(\lambda)}(\mathbf{r}) = \sum_{H' \neq H, \lambda'} \frac{\Phi_{H'(\lambda')}^{(0)}(\mathbf{r})}{E_H^{(0)} - E_{H'}^{(0)}} \langle H'(\lambda') | \delta V_S | H(\lambda) \rangle , \quad (27)$$

and $\langle \mathbf{r} | H(\lambda) \rangle = \Phi_{H(\lambda)}^{(0)}(\mathbf{r})$. Here and in the following, we shall use the Dirac ket to indicate the eigenstate either of a *quantum-mechanical* operator (like $|\mathbf{r}\rangle$, which stands for an eigenstate of the position operator, or $|H(\lambda)\rangle$, sometimes also written as $|nL\rangle$, which stands for an eigenstate of $h_S^{(0)}$) or of a *quantum-field* operator (like $|H(\mathbf{P}, \lambda)\rangle$, which stands for an eigenstate of the pNRQCD Hamiltonian).

In general, δV_S may also depend on the centre-of-mass momentum \mathbf{P} . We shall distinguish between zero-recoil corrections (where δV_S does not depend on \mathbf{P}) and (final-state) recoil corrections (where δV_S depends on \mathbf{P}). Effects of these corrections to the transition amplitude will be discussed in Sec. IV A.

2. Higher Fock-space components

The leading correction to the quarkonium state that accounts for the octet component is induced by

$$\delta H = - \int d^3R \int d^3r \text{Tr} \{ O^\dagger \mathbf{r} \cdot g\mathbf{E} S + S^\dagger \mathbf{r} \cdot g\mathbf{E} O \} . \quad (28)$$

According to the power counting, this is a correction of relative order v . The first-order correction to the quarkonium state is

$$\begin{aligned} |H(\mathbf{P}, \lambda)\rangle^{(1)} = & \int d^3R \int d^3r e^{i\mathbf{P}\cdot\mathbf{R}} \int d^3x \text{Tr} \left\{ O^\dagger(\mathbf{r}, \mathbf{R}) \langle \mathbf{r} | \frac{1}{E_H^{(0)} - h_O^{(0)} - H_{\text{light}}} | \mathbf{x} \rangle \right. \\ & \times \left. [-\mathbf{x} \cdot g\mathbf{E}(\mathbf{R})] \Phi_{H(\lambda)}^{(0)}(\mathbf{x}) |0\rangle \right\} . \end{aligned} \quad (29)$$

Since it has a vanishing projection on $|H(\mathbf{P}, \lambda)\rangle^{(0)}$, in a transition matrix element it contributes at relative order v^2 . Second-order corrections are of relative order v^2 . They contain two orthogonal parts:

$$|H(\mathbf{P}, \lambda)\rangle^{(2)} = |H(\mathbf{P}, \lambda)\rangle_{\perp}^{(2)} + |H(\mathbf{P}, \lambda)\rangle_{\parallel}^{(2)}, \quad (30)$$

where

$$\begin{aligned} |H(\mathbf{P}, \lambda)\rangle_{\perp}^{(2)} &= \int d^3R \int d^3r e^{i\mathbf{P}\cdot\mathbf{R}} \int d^3x \int d^3y \text{Tr} \left\{ S^{\dagger}(\mathbf{r}, \mathbf{R}) \right. \\ &\quad \times \langle \mathbf{r} | \sum_{H' \neq H, \lambda'} \frac{\Phi_{H'(\lambda')}^{(0)}(\mathbf{r}) \Phi_{H'(\lambda')}^{(0)*}(\mathbf{y})}{E_H^{(0)} - E_{H'}^{(0)} - H_{\text{light}}} | \mathbf{y} \rangle [-\mathbf{y} \cdot g \mathbf{E}(\mathbf{R})] \\ &\quad \left. \times \langle \mathbf{y} | \frac{1}{E_H^{(0)} - h_O^{(0)} - H_{\text{light}}} | \mathbf{x} \rangle [-\mathbf{x} \cdot g \mathbf{E}(\mathbf{R})] \Phi_{H(\lambda)}^{(0)}(\mathbf{x}) | 0 \rangle \right\}, \end{aligned} \quad (31)$$

$$|H(\mathbf{P}, \lambda)\rangle_{\parallel}^{(2)} = \frac{\delta Z_{H(\lambda)}}{2} |H(\mathbf{P}, \lambda)\rangle^{(0)}, \quad (32)$$

$$\left(1 + \frac{\delta Z_{H(\lambda)}}{2} \right) (2\pi)^3 \delta^3(\mathbf{P} - \mathbf{P}') = {}^{(0)}\langle H(\mathbf{P}', \lambda) | H(\mathbf{P}, \lambda) \rangle = \sqrt{\frac{\partial E_{H(\lambda)}}{\partial E_H^{(0)}}}. \quad (33)$$

$1 + \delta Z_{H(\lambda)}$ is the usual quantum-mechanical normalization constant of the state, which stands for the probability to find the leading color-singlet component in a physical quarkonium state. Effects of these corrections to the transition amplitude will be discussed in Sec. IV B.

E. M1 transitions in the non-relativistic limit

In accordance with the power counting of pNRQCD, the leading contribution to M1 transitions comes from

$$\mathcal{L}_{\text{M1}}^{(0)} = \int d^3r \text{Tr} \left\{ \frac{1}{2m} V_S^{\frac{\sigma \cdot B}{m}} \{ S^{\dagger}, \boldsymbol{\sigma} \cdot e e_Q \mathbf{B}^{\text{em}} \} S \right\}. \quad (34)$$

As we will discuss in the next section, at leading order $V_S^{\frac{\sigma \cdot B}{m}} = 1$.

For S -wave quarkonium, substituting Eqs. (18), (20), (21) and (34) into Eq. (13) leads to

$$\mathcal{A}^{(0)} [n^3 S_1(\mathbf{0}, \lambda) \rightarrow n'^1 S_0(-\mathbf{k}) \gamma(\mathbf{k}, \sigma)] = \delta_{nn'} i e e_Q \frac{\mathbf{e}_{n^3 S_1}(\lambda) \cdot (\mathbf{k} \times \boldsymbol{\epsilon}^*(\sigma))}{m}, \quad (35)$$

where we have used that

$$\langle \gamma(\mathbf{k}, \sigma) | \mathbf{B}^{\text{em}}(\mathbf{R}) | 0 \rangle = -i \mathbf{k} \times \boldsymbol{\epsilon}^*(\sigma) e^{-i\mathbf{k}\cdot\mathbf{R}}. \quad (36)$$

The factor $\delta_{nn'}$ in Eq. (35) comes from the overlap integral $\int_0^\infty dr r^2 R_{n\ell}(r) R_{n'\ell}(r)$. Substituting the transition amplitude into Eq. (12), we obtain:

$$\Gamma_{n^3S_1 \rightarrow n'^1S_0 \gamma} = \delta_{nn'} \frac{4}{3} \alpha e_Q^2 \frac{k_\gamma^3}{m^2} \left(1 - \frac{k_\gamma}{M_{n^3S_1}} \right). \quad (37)$$

The term $-\delta_{nn'} k_\gamma/M_{n^3S_1}$ is negligible at order $k_\gamma^3 v^2/m^2$: it vanishes for hindered transitions and is of order v^4 for allowed ones. Hence, Eq. (37) gives back Eq. (1) at leading order in the multipole expansion, i.e. the well-known formula of the transition width in the non-relativistic limit.

For P -wave quarkonium we obtain:

$$\mathcal{A}^{(0)} [n^3P_0(\mathbf{0}) \rightarrow n'^1P_1(-\mathbf{k}, \lambda') \gamma(\mathbf{k}, \sigma)] = \delta_{nn'} iee_Q \frac{\mathbf{e}_{n'^1P_1}^*(\lambda') \cdot (\mathbf{k} \times \boldsymbol{\epsilon}^*(\sigma))}{\sqrt{3}m}, \quad (38)$$

$$\begin{aligned} \mathcal{A}^{(0)} [n^3P_1(\mathbf{0}, \lambda) \rightarrow n'^1P_1(-\mathbf{k}, \lambda') \gamma(\mathbf{k}, \sigma)] &= \\ \delta_{nn'} iee_Q \frac{\mathbf{e}_{n'^1P_1}^*(\lambda') \cdot [\mathbf{e}_{n^3P_1}(\lambda) \times (\mathbf{k} \times \boldsymbol{\epsilon}^*(\sigma))]}{\sqrt{2}m}, \end{aligned} \quad (39)$$

$$\begin{aligned} \mathcal{A}^{(0)} [n^3P_2(\mathbf{0}, \lambda) \rightarrow n'^1P_1(-\mathbf{k}, \lambda') \gamma(\mathbf{k}, \sigma)] &= \\ \delta_{nn'} iee_Q \frac{\mathbf{e}_{n'^1P_1}^{*i}(\lambda') h_{n^3P_2}^{ij}(\lambda) (\mathbf{k} \times \boldsymbol{\epsilon}^*(\sigma))^j}{m}. \end{aligned} \quad (40)$$

Substituting the transition amplitudes into Eq. (12), we end up with

$$\Gamma_{n^3P_J \rightarrow n'^1P_1 \gamma} = \delta_{nn'} \frac{4}{3} \alpha e_Q^2 \frac{1}{m^2} k_\gamma^3 \left(1 - \frac{k_\gamma}{M_{n^3P_J}} \right). \quad (41)$$

The width for P -wave spin-singlet to spin-triplet transitions is obtained by multiplying the right-hand side of Eq. (41) by $(2J+1)/3$.

In the following, we will concentrate on higher-order corrections to S -wave transitions. We shall come back to P -wave transitions in Sec. V C.

III. MATCHING OF PNRQCD MAGNETIC DIPOLE OPERATORS

Our aim is to complete Eq. (37) with corrections of relative order v^2 . In accordance with the counting $\alpha_s(m) \sim v^2$ and $\alpha_s(1/r) \sim v$, these also include corrections to the matching coefficients of pNRQCD.

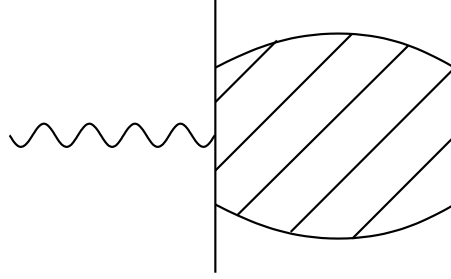


FIG. 2: Green function with four external quark/antiquark lines and a photon. The time flows from the bottom to the top.

The matching coefficients of pNRQCD encode gluons of energy or momentum of order mv . Since this scale is associated with the distance of the two heavy quarks, the matching coefficients are, in general, functions of r . They also contain hard contributions, typically encoded in the matching coefficients inherited from NRQCD. In the following, we will retain the full matching coefficients of NRQCD and count the matching from NRQCD to pNRQCD only in powers of α_s calculated at the soft scale. We will exploit the explicit form of the NRQCD matching coefficients in Secs. V and VI.

The matching from NRQCD to pNRQCD may be performed by calculating Green functions in the two theories and imposing that they are equal order by order in the inverse of the mass and in the multipole expansion. In particular, to match the electromagnetic couplings, we need Green functions with four external quark/antiquark lines and one external photon line as shown in Fig. 2. The matching condition reads:

$$G_\gamma^{\text{NRQCD}}(x'_1, x'_2, x_1, x_2) = G_\gamma^{\text{pNRQCD}}(x'_1, x'_2, x_1, x_2). \quad (42)$$

Since we are working in a situation where the typical momentum transfer between the heavy quarks is larger than Λ_{QCD} , we may, in addition, perform the matching order by order in α_s .

A. Matching at $\mathcal{O}(1)$

If we aim at calculating the matching at $\mathcal{O}(1)$ a convenient approach consists in projecting NRQCD on the two-quark Fock space spanned by

$$\int d^3x_1 d^3x_2 \psi^\dagger(\mathbf{x}_1, t) \varphi(\mathbf{x}_1, \mathbf{x}_2, t) \chi(\mathbf{x}_2, t) |0\rangle, \quad (43)$$

where $\varphi(\mathbf{x}_1, \mathbf{x}_2, t)$ is a $3 \otimes 3$ tensor in color space and a $2 \otimes 2$ tensor in spin space. After projection, all gluon fields are multipole expanded in \mathbf{r} . Gauge invariance is made explicit at the Lagrangian level by decomposing

$$\begin{aligned} \varphi(\mathbf{x}_1, \mathbf{x}_2, t) &= P \exp \left(ig \int_{x_1}^{x_2} \mathbf{A} \cdot d\mathbf{x} \right) S'(\mathbf{R}, \mathbf{r}, t) \\ &\quad + P \exp \left(ig \int_{\mathbf{R}}^{x_1} \mathbf{A} \cdot d\mathbf{x} \right) O'(\mathbf{R}, \mathbf{r}, t) \exp \left(ig \int_{x_2}^{\mathbf{R}} \mathbf{A} \cdot d\mathbf{x} \right), \end{aligned} \quad (44)$$

$$S'(\mathbf{R}, \mathbf{r}, t) = \exp \left(iee_Q \int_{x_1}^{x_2} \mathbf{A}^{\text{em}} \cdot d\mathbf{x} \right) S(\mathbf{R}, \mathbf{r}, t), \quad (45)$$

$$O'(\mathbf{R}, \mathbf{r}, t) = \exp \left(iee_Q \int_{x_1}^{x_2} \mathbf{A}^{\text{em}} \cdot d\mathbf{x} \right) O(\mathbf{R}, \mathbf{r}, t), \quad (46)$$

where P stands for path ordering, $\mathbf{R} = (\mathbf{x}_1 + \mathbf{x}_2)/2$ and $\mathbf{r} = \mathbf{x}_1 - \mathbf{x}_2$. The fields S and O transform like singlets under $U(1)_{\text{em}}$ gauge transformations and like singlet and octet respectively under $SU(3)_c$ gauge transformations. After projecting (2) on (43), one obtains

$$V_A^{\text{em}} = 1, \quad (47)$$

$$V_S^{\frac{\sigma \cdot B}{m}} = c_F^{\text{em}}, \quad (48)$$

$$V_S^{(r \cdot \nabla)^2 \frac{\sigma \cdot B}{m}} = c_F^{\text{em}}, \quad (49)$$

$$V_O^{\frac{\sigma \cdot B}{m}} = c_F^{\text{em}}, \quad (50)$$

$$V_S^{\frac{\sigma \cdot \nabla \times E}{m^2}} = c_S^{\text{em}}, \quad (51)$$

$$V_S^{\frac{\sigma \cdot \nabla_r \times r \cdot \nabla E}{m^2}} = c_S^{\text{em}}, \quad (52)$$

$$V_S^{\frac{\nabla_r^2 \sigma \cdot B}{m^3}} = c_{W1}^{\text{em}} - c_{W2}^{\text{em}} = 1, \quad (53)$$

$$V_S^{\frac{(\nabla_r \cdot \sigma)(\nabla_r \cdot B)}{m^3}} = c_{p'p}^{\text{em}}. \quad (54)$$

The matching coefficients $V_S^{\frac{\sigma \cdot (r \times r \times B)}{m^2}}$ and $V_S^{\frac{\sigma \cdot B}{m^2}}$ are zero at $\mathcal{O}(1)$.

We consider now the impact of the $\mathcal{O}(1)$ matching on the transition amplitude. In order to keep the notation compact, it is useful to define

$$\bar{\mathcal{A}} \equiv \frac{\mathcal{A}}{\bar{\mathcal{A}}^{(0)}}, \quad (55)$$

where \mathcal{A} is an amplitude calculated from Eq. (13) by substituting $\mathcal{L}_{\gamma p \text{NRQCD}}$ with the considered operator and $\bar{\mathcal{A}}^{(0)}$ is connected with the leading M1 amplitude $\mathcal{A}^{(0)}$ (35) by

$$\delta_{nn'} \bar{\mathcal{A}}^{(0)} \equiv \mathcal{A}^{(0)}. \quad (56)$$

(A) The matching coefficient (48) induces the following correction to $\mathcal{A}^{(0)}$:

$$\overline{\mathcal{A}} [n^3 S_1(\mathbf{0}, \lambda) \rightarrow n'^1 S_0(-\mathbf{k}) \gamma(\mathbf{k}, \sigma)] = \kappa_Q^{\text{em}} \delta_{nn'} . \quad (57)$$

(B) The correction induced by the operator $\frac{c_F^{\text{em}}}{16m} \{S^\dagger, \mathbf{r}^i \mathbf{r}^j (\nabla^i \nabla^j \boldsymbol{\sigma} \cdot ee_Q \mathbf{B}^{\text{em}})\} S$ is

$$\overline{\mathcal{A}} [n^3 S_1(\mathbf{0}, \lambda) \rightarrow n'^1 S_0(-\mathbf{k}) \gamma(\mathbf{k}, \sigma)] = -\frac{c_F^{\text{em}}}{24} k^2 \langle n' S | \mathbf{r}^2 | n S \rangle . \quad (58)$$

(C) The correction induced by the operator $-\frac{c_S^{\text{em}}}{16m^2} [S^\dagger, \boldsymbol{\sigma} \cdot [-i \nabla \times, ee_Q \mathbf{E}^{\text{em}}]] S$ is

$$\overline{\mathcal{A}} [n^3 S_1(\mathbf{0}, \lambda) \rightarrow n'^1 S_0(-\mathbf{k}) \gamma(\mathbf{k}, \sigma)] = c_S^{\text{em}} \frac{k}{8m} \delta_{nn'} , \quad (59)$$

where we have used

$$\langle \gamma(\mathbf{k}, \sigma) | \mathbf{E}^{\text{em}}(\mathbf{R}) | 0 \rangle = -ik \boldsymbol{\epsilon}^*(\sigma) e^{-i\mathbf{k} \cdot \mathbf{R}} . \quad (60)$$

(D) The correction induced by the operator $-\frac{c_S^{\text{em}}}{16m^2} [S^\dagger, \boldsymbol{\sigma} \cdot [-i \nabla_r \times, \mathbf{r}^i (\nabla^i ee_Q \mathbf{E}^{\text{em}})]] S$ is

$$\overline{\mathcal{A}} [n^3 S_1(\mathbf{0}, \lambda) \rightarrow n'^1 S_0(-\mathbf{k}) \gamma(\mathbf{k}, \sigma)] = c_S^{\text{em}} \frac{k}{8m} \left(\delta_{nn'} + i \frac{2}{3} \langle n' S | \mathbf{r} \cdot \mathbf{p} | n S \rangle \right) . \quad (61)$$

(E) The correction induced by the operator $\frac{1}{4m^3} \{S^\dagger, \boldsymbol{\sigma} \cdot ee_Q \mathbf{B}^{\text{em}}\} \nabla_r^2 S$ is

$$\overline{\mathcal{A}} [n^3 S_1(\mathbf{0}, \lambda) \rightarrow n'^1 S_0(-\mathbf{k}) \gamma(\mathbf{k}, \sigma)] = -\langle n' S | \frac{\mathbf{p}^2}{2m^2} | n S \rangle . \quad (62)$$

(F) The correction induced by the operator $\frac{c_{p'p}^{\text{em}}}{8m^3} \{S^\dagger, \boldsymbol{\sigma}^i ee_Q \mathbf{B}^{\text{em}j}\} \nabla_r^i \nabla_r^j S$ is

$$\overline{\mathcal{A}} [n^3 S_1(\mathbf{0}, \lambda) \rightarrow n'^1 S_0(-\mathbf{k}) \gamma(\mathbf{k}, \sigma)] = -\frac{\kappa_Q^{\text{em}}}{3} \langle n' S | \frac{\mathbf{p}^2}{2m^2} | n S \rangle , \quad (63)$$

where we have used $c_{p'p}^{\text{em}} = \kappa_Q^{\text{em}}$.

B. Calculation of $V_S^{\frac{\sigma \cdot B}{m}}$

In this section, we match the operator (34) beyond $\mathcal{O}(1)$. This operator provides the leading transition widths (37) and (41) in the case of allowed M1 transitions. Hence, corrections of order α_s and α_s^2 to $V_S^{\frac{\sigma \cdot B}{m}}$, which may arise in the matching from NRQCD to pNRQCD, are potentially larger than or of the same order as genuine relativistic v^2 corrections to the

transition width. Surprisingly, we shall be able to perform the matching exactly and provide a result that is valid to all orders in perturbation theory and non-perturbatively.

Before going to the matching, we recall that the matching coefficient c_F^{em} that appears in the NRQCD Lagrangian (2) is the heavy-quark magnetic moment. The matching coefficient $V_S^{\frac{\sigma \cdot B}{m}}$ is the magnetic moment of the singlet-quarkonium field. While the first one gets only contributions from the hard modes, the second one may potentially get large contributions stemming from the soft scale.

The matching of $V_S^{\frac{\sigma \cdot B}{m}}$ proceeds as follows.

(1) First, we note that the only amplitudes in NRQCD that may contribute to the matching are those where the photon couples to the heavy quark (antiquark) through the operators $\psi^\dagger \boldsymbol{\sigma} \cdot ee_Q \mathbf{B}^{\text{em}} \psi / m$ or $-\chi^\dagger \boldsymbol{\sigma} \cdot ee_Q \mathbf{B}^{\text{em}} \chi / m$. At order $1/m$, this is the only magnetic spin-flipping coupling to the quark. If the photon couples to loops of massless quarks then, at leading order in the electromagnetic coupling constant, the sum of the electric charges over three light flavors vanishes. In the bottomonium system, contributions from charm-quark loops should also be considered. If the momentum flowing through the loop is hard, the contribution is suppressed by, at least, $\alpha_s^2(m_b)$ and, therefore, beyond the accuracy of this work. If the momentum is soft, the charm quark effectively decouples and the system can be described by an effective field theory with three massless quarks [24, 25].

(2) The crucial point is to recognize that there are no extra momentum or spin dependent insertions on the heavy-quark lines that contribute to the matching of $V_S^{\frac{\sigma \cdot B}{m}}$, since they carry extra $1/m$ suppressions. As a consequence, the magnetic spin-flipping operator $\boldsymbol{\sigma} \cdot ee_Q \mathbf{B}^{\text{em}} / m$ behaves, for the purpose of the matching, as the identity operator in coordinate space⁴ and the magnetic matrix element factorizes. Therefore, any (normalized) NRQCD amplitude contributing to $V_S^{\frac{\sigma \cdot B}{m}}$ may be written as

$$\frac{c_F^{\text{em}}}{2m} \int_{t_i}^{t_f} dt \langle \gamma | \boldsymbol{\sigma}^{(1)} \cdot ee_Q \mathbf{B}^{\text{em}}(\mathbf{x}_1, t) + \boldsymbol{\sigma}^{(2)} \cdot ee_Q \mathbf{B}^{\text{em}}(\mathbf{x}_2, t) | 0 \rangle, \quad (64)$$

which, after multipole expansion of the magnetic field, becomes (we neglect terms propor-

⁴ The property that $\boldsymbol{\sigma} \cdot ee_Q \mathbf{B}^{\text{em}} / m$ depends neither on gluon fields nor on the relative coordinate \mathbf{r} , which in turn is a consequence of the ultrasoft nature of the external photon, will be used again and again in the course of the paper and is at the origin of most results.

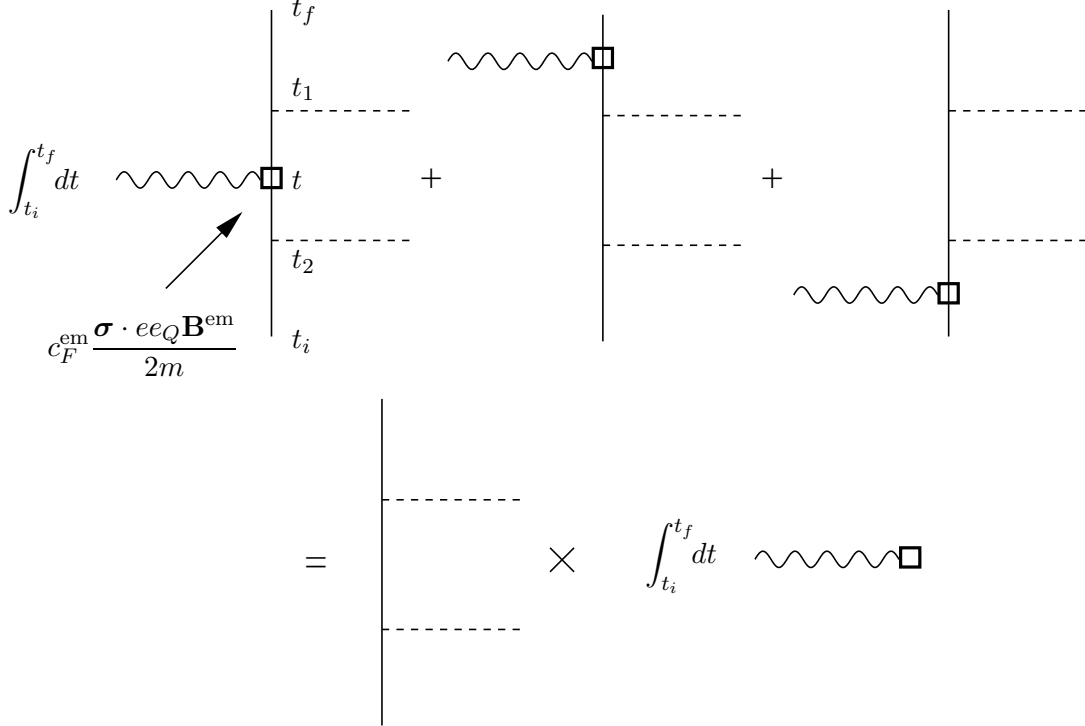


FIG. 3: Diagrammatic factorization of the magnetic dipole coupling in static NRQCD: $t_f > t_1 > t_2 > t_i$. Dashed lines are longitudinal gluons, the box represents the magnetic dipole coupling.

tional to \mathbf{r}):

$$\left(\frac{c_F^{\text{em}}}{2m} + \frac{c_F^{\text{em}}}{16m} (\mathbf{r} \cdot \nabla)^2 + \dots \right) (\boldsymbol{\sigma}^{(1)} + \boldsymbol{\sigma}^{(2)}) \cdot \int_{t_i}^{t_f} dt \langle \gamma | ee_Q \mathbf{B}^{\text{em}}(t) | 0 \rangle, \quad (65)$$

where $\boldsymbol{\sigma}^{(1)}$ stands for the Pauli matrices acting on the quark and $\boldsymbol{\sigma}^{(2)}$ for the Pauli matrices acting on the antiquark.

To see how factorization works from a diagrammatic point of view, let us consider a photon insertion on a quark line. In general, this happens in between two longitudinal gluon insertions (first diagram of Fig. 3). Transverse gluons couple to quark lines through $1/m$ suppressed operators and are irrelevant for the purpose of the matching. At order $1/m^0$, the coupling of longitudinal gluons to quark lines is spin and momentum independent. Therefore, $\boldsymbol{\sigma} \cdot ee_Q \mathbf{B}^{\text{em}}$ may be freely moved along the quark lines. The sum of the first three diagrams of Fig. 3 is proportional to

$$\begin{aligned} & \theta(t_f - t_1) \theta(t_1 - t) \theta(t - t_2) \theta(t_2 - t_i) + \theta(t_f - t) \theta(t - t_1) \theta(t_1 - t_2) \theta(t_2 - t_i) \\ & + \theta(t_f - t_1) \theta(t_1 - t_2) \theta(t_2 - t) \theta(t - t_i) \\ & = \theta(t_f - t) \theta(t - t_i) \theta(t_f - t_1) \theta(t_1 - t_2) \theta(t_2 - t_i), \end{aligned}$$

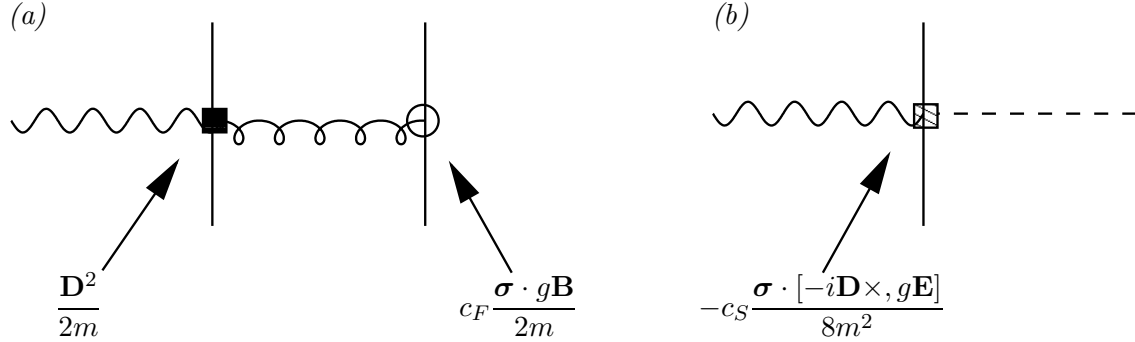


FIG. 4: Diagrams contributing at order α_s to $V_S^{\frac{\sigma \cdot (r \times r \times B)}{m^2}}$. Although not displayed, the symmetric diagrams are understood. \mathbf{D} is the covariant derivative under $SU(3)_c \times U(1)_{\text{em}}$.

where the thetas come from the static heavy-quark propagators. The equality completes the factorization proof graphically represented in Fig. 3.

(3) By matching Eq. (65) to the pNRQCD amplitude

$$\left(\frac{V_S^{\frac{\sigma \cdot B}{m}}}{2m} + \frac{V_S^{(r \cdot \nabla)^2 \frac{\sigma \cdot B}{m}}}{16m} (\mathbf{r} \cdot \nabla)^2 + \dots \right) (\boldsymbol{\sigma}^{(1)} + \boldsymbol{\sigma}^{(2)}) \cdot \int_{t_i}^{t_f} dt \langle \gamma | e e_Q \mathbf{B}^{\text{em}}(t) | 0 \rangle, \quad (66)$$

it follows that

$$V_S^{\frac{\sigma \cdot B}{m}} = V_S^{(r \cdot \nabla)^2 \frac{\sigma \cdot B}{m}} = c_F^{\text{em}}. \quad (67)$$

Equation (67) is a result that holds to all orders in the strong-coupling constant and also non-perturbatively. It excludes that the $1/m$ magnetic coupling of the quarkonium field is affected by any soft contribution. A fortiori, it excludes large anomalous non-perturbative corrections to this coupling.

C. Calculation of $V_S^{\frac{\sigma \cdot (r \times r \times B)}{m^2}}$ and $V_S^{\frac{\sigma \cdot B}{m^2}}$

The matching coefficients $V_S^{\frac{\sigma \cdot (r \times r \times B)}{m^2}}$ and $V_S^{\frac{\sigma \cdot B}{m^2}}$ do not get contributions at $\mathcal{O}(1)$. At order α_s , the diagrams contributing to the NRQCD part of the matching are shown in Fig 4. Note that the photon is emitted by the electromagnetic field embedded in the covariant derivative. If we sandwich the diagrams between initial and final states that are gauge invariant under $SU(3)_c \times U(1)_{\text{em}}$ and multipole expand the external electromagnetic field, we obtain:

$$V_S^{\frac{\sigma \cdot (r \times r \times B)}{m^2}} = \frac{C_F \alpha_s}{2} (2c_F - c_S) = \frac{C_F \alpha_s}{2}, \quad (68)$$

$$V_S^{\frac{\sigma \cdot B}{m^2}} = 0. \quad (69)$$

In the first equation, we have made use of Eq. (4). Alternatively, we may first perform the matching in a non explicitly gauge-invariant fashion, as it is customary in perturbative calculations of Green functions, and then impose gauge invariance at the level of the pNRQCD Lagrangian through field redefinitions of the type (44)-(46).

Equation (68) may be generalized to all orders as

$$V_S^{\frac{\sigma \cdot (r \times r \times B)}{m^2}} = \frac{r^2 V_S^{(0)'} }{2}, \quad (70)$$

where $V_S^{(0)'}$ stands for $dV_S^{(0)} / dr$. Also Eq. (69) is valid to all orders. The proof proceeds as follows.

(1) The matching can be performed order by order in $1/m$. NRQCD amplitudes that may contribute to the matching involve either insertions of two of the operators $\mathbf{D}^2/2m$, $c_F \boldsymbol{\sigma} \cdot g\mathbf{B}/2m$ and $c_F^{\text{em}} \boldsymbol{\sigma} \cdot ee_Q \mathbf{B}^{\text{em}}/2m$, or one insertion of the operator $-c_s \boldsymbol{\sigma} \cdot [-i\mathbf{D} \times, g\mathbf{E}]/8m^2$ on either the quark or the antiquark line. Couplings of the photon to massless quark loops or charm-quark loops may be neglected by the same arguments given in the previous section for the matching of $V_S^{\frac{\sigma \cdot B}{m}}$.

(2) First, we consider amplitudes with an insertion of the operator $c_F^{\text{em}} \boldsymbol{\sigma} \cdot ee_Q \mathbf{B}^{\text{em}}/2m$ and one of either $\mathbf{D}^2/2m$ or $c_F \boldsymbol{\sigma} \cdot g\mathbf{B}/2m$. In the first case, due to the ultrasoft nature of the external photon, we may neglect the action of ∇ on \mathbf{B}^{em} . Hence the magnetic dipole operator behaves like the identity operator, and, following an argument similar to that one developed in the previous section, we can show that there is no contribution to the matching. In the second case, the QCD part of the amplitude factorizes in a term proportional to the expectation value of the chromomagnetic operator, which vanishes for parity.

(3) In all the remaining terms, the electromagnetic coupling is embedded in a covariant derivative. Since by projecting the operator

$$\int d^3x \psi^\dagger (-i\nabla - ee_Q \mathbf{A}^{\text{em}}) \psi + [\psi \rightarrow i\sigma^2 \chi^*], \quad (71)$$

onto the state (43) and taking into account gauge invariance (see Eq. (45)) we obtain⁵

$$\int d^3R d^3r \text{Tr} \left\{ \mathbf{S}^\dagger \left(-i\nabla + \mathbf{r} \times ee_Q \mathbf{B}^{\text{em}} + \mathcal{O}(r^2) \right) \mathbf{S} \right\},$$

⁵ From

$$\exp \left(-iee_Q \int_{x_1}^{x_2} \mathbf{A}^{\text{em}} \cdot d\mathbf{x} \right) [-i\nabla_{x_1} - ee_Q \mathbf{A}(x_1) - i\nabla_{x_2} + ee_Q \mathbf{A}(x_2)] \exp \left(iee_Q \int_{x_1}^{x_2} \mathbf{A}^{\text{em}} \cdot d\mathbf{x} \right)$$

and multipole expanding one ends up with $-i\nabla + \mathbf{r} \times ee_Q \mathbf{B}^{\text{em}} + \mathcal{O}(r^2)$.

we conclude that the matching coefficients of the operators

$$\frac{1}{4m^2 r^3} \{S^\dagger, \boldsymbol{\sigma} \cdot [\mathbf{r} \times (\mathbf{r} \times ee_Q \mathbf{B}^{\text{em}})]\} S \quad (72)$$

and

$$\frac{1}{4m^2 r^3} \{S^\dagger, \boldsymbol{\sigma}\} \cdot [\mathbf{r} \times (-i\boldsymbol{\nabla})] S \quad (73)$$

are equal. Indeed, the first is obtained from the second by replacing $-i\boldsymbol{\nabla}$ by $\mathbf{r} \times ee_Q \mathbf{B}^{\text{em}}$. The operator $\frac{1}{4m^2 r^3} \{S^\dagger, \boldsymbol{\sigma}\} \cdot [\mathbf{r} \times (-i\boldsymbol{\nabla})] S$ is protected by Poincaré invariance (Gromes relation) [26, 27, 28]. Its matching coefficient is equal to $r^2 V_S^{(0)}/2$ to all orders of perturbation theory and non-perturbatively. This proves Eq. (70). It also proves Eq. (69), because the analysis does not reveal any contribution to $V_S^{\frac{\sigma \cdot \mathbf{B}}{m^2}}$.

Equations (70) and (69) are both valid to all orders in perturbation theory and non-perturbatively. The first equation confirms earlier findings in phenomenological models (see, for instance, [12]). The second one states that to all orders in the strong-coupling constant and non-perturbatively the existence of a magnetic coupling of the type induced by a scalar interaction is excluded. Phenomenological models often assume that the relativistic Hamiltonian contains a scalar interaction $\gamma^{0(1)} V^{\text{scalar}}(r) \gamma^{0(2)}$. The non-relativistic reduction of this term generates, among others, a magnetic spin-flipping term of the type $\frac{1}{2m^2} V^{\text{scalar}} \{S^\dagger, \boldsymbol{\sigma} \cdot ee_Q \mathbf{B}^{\text{em}}\} S$. Our analysis shows that such a term is excluded from pNRQCD. We conclude that a scalar interaction would induce a M1 coupling that in QCD cannot be generated, even dynamically, for heavy-quark bound state systems.⁶

The correction induced by the operator

$$\frac{1}{4m^2} \frac{r V_S^{(0)'}(r)}{2} \{S^\dagger, \boldsymbol{\sigma} \cdot [\hat{\mathbf{r}} \times (\hat{\mathbf{r}} \times ee_Q \mathbf{B}^{\text{em}})]\} S \quad (74)$$

to the M1 transition amplitude is

$$\bar{\mathcal{A}} [n^3 S_1(\mathbf{0}, \lambda) \rightarrow n' 1 S_0(-\mathbf{k}) \gamma(\mathbf{k}, \sigma)] = -\frac{1}{6m} \langle n' S | r V_S^{(0)'} | n S \rangle. \quad (75)$$

Finally, we note that amplitudes with one insertion of the operator $-c_S^{\text{em}} \boldsymbol{\sigma} \cdot [-i\boldsymbol{\nabla} \times, ee_Q \mathbf{E}^{\text{em}}]/8m^2$ only contribute to the matching of $V_S^{\frac{\sigma \cdot \nabla \times E}{m^2}}$ and $V_S^{\frac{\sigma \cdot \nabla r \times r \cdot \nabla E}{m^2}}$. Since the operator factorizes, there are no soft contributions to the matching coefficients and Eqs. (51) and (52) turn out to be valid to all orders in α_s .

⁶ The situation is here different from the case of the spin-dependent potentials. There, a spin-orbit potential of the type induced by a scalar interaction may be dynamically generated [29, 30]. The particular nature of the scalar interaction contribution to M1 transitions has also been discussed in [31].

D. Comment on the matching in the strong-coupling regime

In the weak-coupling regime, at relative order v^2 , the only $1/m^3$ operator relevant for M1 transitions is

$$\frac{1}{4m^3} \left\{ S^\dagger, \boldsymbol{\sigma} \cdot ee_Q \mathbf{B}^{\text{em}} \right\} \nabla_r^2 S.$$

Note that loop corrections to the matching coefficient are suppressed by powers of $\alpha_s(1/r) \ll 1$ and all other possible $1/m^3$ operators are suppressed by powers of α_s .

Comparing our expression of the pNRQCD Lagrangian (10) with the phenomenological Hamiltonian used in [12], we observe that, up to the scalar interaction term, the two expressions are equal. The absence of a scalar interaction in pNRQCD has been discussed above. Here, we remark that our expression is valid in the weak-coupling regime ($mv^2 \gtrsim \Lambda_{\text{QCD}}$) only, while phenomenological Hamiltonians are supposed to be applicable to both weakly and strongly coupled quarkonia. We may ask how the pNRQCD Lagrangian would change in the strong-coupling regime ($mv \sim \Lambda_{\text{QCD}}$). This has been discussed in the absence of an electromagnetic interaction in [30, 32, 33, 34, 35]. Here, we focus on the magnetic dipole couplings. We have shown that the $1/m$ and $1/m^2$ matching is valid beyond perturbation theory. However, this is unlikely to happen at order $1/m^3$. Since $\alpha_s(1/r) \sim 1$ is no longer a suppression factor, we expect more NRQCD amplitudes to contribute to the matching. Among them, we may have amplitudes made of two insertions of the operator $c_F \boldsymbol{\sigma} \cdot g\mathbf{B}/2m$ and one of $c_F^{\text{em}} \boldsymbol{\sigma} \cdot ee_Q \mathbf{B}^{\text{em}}/2m$, or one of $-c_s \boldsymbol{\sigma} \cdot [-i\mathbf{D} \times, g\mathbf{E}]/8m^2$ and one of $\mathbf{D}^2/2m$, or one of $-c_s \boldsymbol{\sigma} \cdot [-i\mathbf{D} \times, g\mathbf{E}]/8m^2$ and one of $c_F \boldsymbol{\sigma} \cdot g\mathbf{B}/2m$ and so on. These amplitudes will be encoded in the matching coefficients of pNRQCD in the form of static Wilson loop amplitudes with field strength insertions of the same kind as those that appear in the QCD potential at order $1/m^2$ [30]. Also, they may induce new operators in pNRQCD. A non-perturbative derivation of the pNRQCD Lagrangian coupled to the electromagnetic field at order $1/m^3$ has not been worked out. In a purely analytical approach, such a computation will likely have a limited phenomenological impact, due to the many non-perturbative parameters (Wilson-loop amplitudes) needed. However, if supplemented by lattice simulations, it will pave the way to a rigorous QCD study of relativistic corrections to M1 transitions in excited heavy-quarkonium states.

In summary, phenomenological models used so far to describe magnetic dipole transitions in quarkonium, once cleaned of the scalar interaction, appear to be valid only for

weakly-coupled resonances. For strongly-coupled resonances, at order $1/m^3$, more terms and matching coefficients with, in principle, large non-perturbative corrections are expected.

IV. WAVE-FUNCTION CORRECTIONS TO MAGNETIC DIPOLE TRANSITIONS

Corrections to the wave function that give contributions of relative order v^2 to the transition amplitude are of two categories: (A) higher-order potential corrections, which may be further distinguished in (A.1) zero-recoil corrections and (A.2) recoil effects of the final-state quarkonium, and (B) higher Fock-state corrections.

A. Corrections to the wave function from higher-order potentials

1. Zero-recoil effects

We first consider corrections coming from higher-order potentials that do not depend on the centre-of-mass momentum of the recoiling quarkonium. Since δV_S is, at least, of order v^4 , we only need to take into account the correction induced by Eq. (27) to the leading amplitude computed in Sec. II E. The correction is proportional to

$$(1 - \delta_{n'n}) \langle n'S | \text{Tr} \{ \{ \boldsymbol{\sigma}, \delta V_S \mathbf{e}_{n^3 S_1}(\lambda) \cdot \boldsymbol{\sigma} \} - \delta V_S \{ \boldsymbol{\sigma}, \mathbf{e}_{n^3 S_1}(\lambda) \cdot \boldsymbol{\sigma} \} \} | nS \rangle.$$

It vanishes for allowed magnetic transitions. This follows from the fact that $\boldsymbol{\sigma} \cdot e e_Q \mathbf{B}^{\text{em}}/m$ is independent of \mathbf{r} and the first-order correction is orthogonal to the zeroth-order wave function (see Eq. (27)). The two terms in the trace come from the correction to the incoming and outgoing heavy quarkonium respectively. We distinguish different cases. (i) If δV_S is spin independent, then the trace vanishes. (ii) If δV_S is a spin-orbit potential, then $\langle n'S | \delta V_S | nS \rangle \sim \langle n'S | \mathbf{r} \times \mathbf{p} | nS \rangle = 0$ on S waves. (iii) If δV_S is a spin-tensor potential, then $\langle n'S | \delta V_S | nS \rangle \sim \langle n'S | 3\mathbf{r}^i \mathbf{r}^j - r^2 \delta^{ij} | nS \rangle = 0$ on S waves. (iv) The only non-vanishing contribution comes from the spin-spin potential:

$$\text{Tr} \{ S^\dagger \delta V_S S \} = -\frac{V^{\text{ss}}(\mathbf{r})}{4m^2} \text{Tr} \{ S^\dagger \boldsymbol{\sigma}^i S \boldsymbol{\sigma}^i \}. \quad (76)$$

It induces the following correction to the transition amplitude:

$$\overline{\mathcal{A}} [n^3 S_1(\mathbf{0}, \lambda) \rightarrow n'^1 S_0(-\mathbf{k}) \gamma(\mathbf{k}, \sigma)] = c_F^{\text{em}} (1 - \delta_{n'n}) \frac{1}{m^2} \frac{\langle n'S | V^{\text{ss}}(\mathbf{r}) | nS \rangle}{E_n^{(0)} - E_{n'}^{(0)}}. \quad (77)$$

The correction is only relevant for hindered M1 transitions and, in this case, is of order v^2 ($V^{\text{ss}}/(E_n^{(0)} - E_{n'}^{(0)}) \sim mv^4/mv^2 \sim v^2$).

2. Final-state recoil effects

The final-state quarkonium is not at rest. It moves with a velocity $-\mathbf{k}$ with respect to the centre-of-mass frame. In [12], it has been pointed out that due to this motion, higher-order potentials that depend on the centre-of-mass momentum may modify the wave function of the recoiling quarkonium such that the E1 operator may induce an effective M1 transition. The leading potential relevant to our case is:

$$\text{Tr} \{ S^\dagger \delta V_S S \} = -\frac{1}{4m^2} \frac{V_S^{(0)'} }{2} \text{Tr} \{ \{ S^\dagger, \boldsymbol{\sigma} \} \cdot [\hat{\mathbf{r}} \times (-i\boldsymbol{\nabla})] S \} . \quad (78)$$

We have discussed the spin-orbit potential in Sec. III C (see Eq. (73)), where we noticed that its value is protected by Poincaré invariance. Inserting Eq. (78) into Eqs. (26) and (27) we obtain

$$|H(\mathbf{P}, \lambda)\rangle^{(1)} = - \int d^3R \int d^3r e^{i\mathbf{P}\cdot\mathbf{R}} \text{Tr} \left\{ \frac{\mathbf{P}}{8m^2} \cdot \{ S^\dagger, \boldsymbol{\sigma} \} \times (\boldsymbol{\nabla}_r \Phi_{H(\lambda)}) |0\rangle \right\} , \quad (79)$$

where we have used

$$\frac{1}{E_H^{(0)} - E_{H'}^{(0)}} \langle H'(\lambda') | \hat{\mathbf{r}} V_S^{(0)'} | H(\lambda) \rangle = i \langle H'(\lambda') | \mathbf{p} | H(\lambda) \rangle ,$$

which follows from $[\mathbf{p}, h_S^{(0)}] = -i\hat{\mathbf{r}} V_S^{(0)'}(r)$, and

$$\sum_{H' \neq H, \lambda'} \Phi_{H'(\lambda')}^{(0)}(\mathbf{r}) i \langle H'(\lambda') | \mathbf{p} | H(\lambda) \rangle = \boldsymbol{\nabla}_r \Phi_{H(\lambda)}^{(0)}(\mathbf{r}) ,$$

which follows from completeness and the definite parity of the functions $\Phi_{H(\lambda)}^{(0)}$. Two different derivations of Eq. (79), one that uses Lorentz-boost transformations and another one based on relativistically covariant formulations, can be found in Appendix A.

Equation (79) states that, due to the recoil, the final state develops a nonzero P -wave, spin-flipped, component suppressed by a factor $v k_\gamma / m$. As a consequence, in a $n^3S_1 \rightarrow n'^1S_0 \gamma$ transition, the P -wave spin-triplet final state component can be reached from the initial 3S_1 state through an E1 transition, mediated by the operator

$$\mathcal{L}_{\text{E1}}^{(0)} = \int d^3r \text{Tr} \{ S^\dagger \mathbf{r} \cdot ee_Q \mathbf{E}^{\text{em}} S \} . \quad (80)$$

Since the E1 operator is enhanced by $1/v$ relative to the leading M1 operator (34), the recoil correction is of order k_γ/m with respect to the leading term. At relative order v^2 , this correction is negligible for M1 allowed transitions ($k_\gamma \ll mv^2$), but should be considered for M1 hindered transitions, where $k_\gamma \sim mv^2$.⁷

The correction to the transition amplitude is given by

$$- \langle^{(1)} n'{}^1S_0(-\mathbf{k}) \gamma(\mathbf{k}, \sigma) | \int d^3R \mathcal{L}_{\text{E1}}^{(0)} | n^3S_1(\mathbf{0}, \lambda) \rangle, \quad (81)$$

where $|n'{}^1S_0(-\mathbf{k})\rangle^{(1)}$ can be inferred from Eq. (79). After a straightforward calculation, we obtain

$$\overline{\mathcal{A}} [n^3S_1(\mathbf{0}, \lambda) \rightarrow n'{}^1S_0(-\mathbf{k}) \gamma(\mathbf{k}, \sigma)] = \frac{k}{4m} \left(\delta_{n'n} + \frac{i}{3} \langle n'{}^1S | \mathbf{r} \cdot \mathbf{p} | n{}^3S \rangle \right). \quad (82)$$

B. Color-octet effects

In Sec. II D 2, we pointed out that a heavy quarkonium state also contains higher Fock components, in particular, components made of a quark-antiquark pair in an octet configuration. Color-octet effects are regarded as one of the most distinctive benchmarks of NRQCD, and have been found to play a crucial role in several phenomenological applications, e.g. heavy quarkonium decays and productions [2]. Indeed, color-octet effects are not included in any potential-model formulation and have not been considered so far in radiative transitions. A color-singlet quarkonium may develop a color-octet component by emitting and reabsorbing an ultrasoft gluon. A M1 transition may occur either in the color-singlet or in the color-octet component. If $\Lambda_{\text{QCD}} \sim mv^2$, the process involving a singlet-octet-singlet transition is suppressed only by a factor v^2 with respect to the leading one, and, therefore, relevant to our analysis.

In [4, 36], the effect of octet components to the spectrum has been thoroughly investigated. The leading effect is given by⁸

$$\delta E_{H(\lambda)} = \frac{i}{6} \int_0^\infty dt \langle 0 | g \mathbf{E}^a(\mathbf{R}, 0) \phi(0, t)_{ab}^{\text{adj}} g \mathbf{E}^b(\mathbf{R}, t) | 0 \rangle \langle H(\lambda) | \mathbf{r} e^{-i(E_H^{(0)} - h_O^{(0)})t} \mathbf{r} | H(\lambda) \rangle. \quad (83)$$

⁷ In the gauge non-invariant formulation of Appendix B, the leading E1 operator is given by Eq. (B3). At relative order v^2 , it contributes both to allowed and hindered transitions.

⁸ Note that in [4, 36] a different normalization for the state $|0\rangle$ is used: $|0\rangle = |0\rangle_{[4, 36]} / \sqrt{N_c}$.

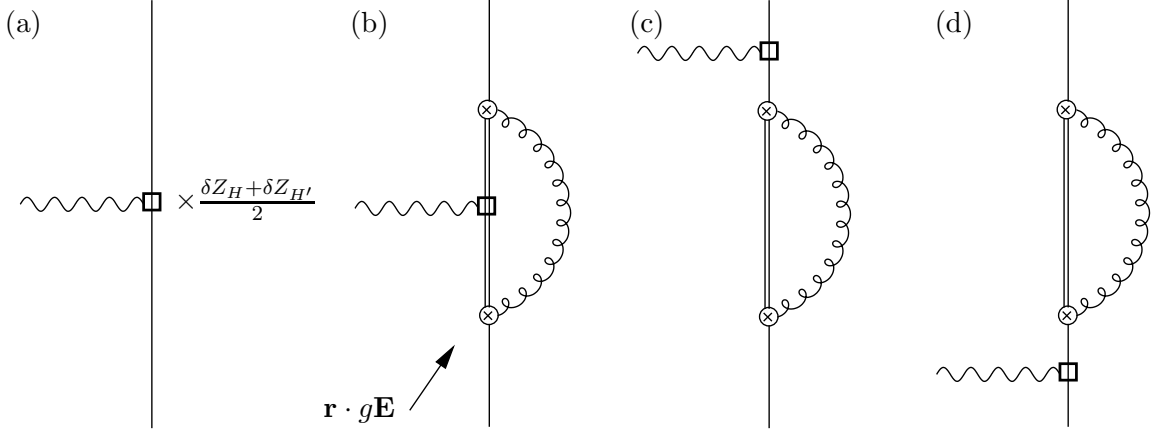


FIG. 5: Octet contributions to M1 transitions. The single and double lines represent the singlet and octet fields, respectively. The circled cross stands for the vertex induced by the interaction (28).

Note the appearance of the non-local condensate $\langle 0 | g\mathbf{E}^a(\mathbf{R}, 0) \phi(0, t)_{ab}^{\text{adj}} g\mathbf{E}^b(\mathbf{R}, t) | 0 \rangle$, typical of the situation $\Lambda_{\text{QCD}} \sim mv^2$. $\phi(0, t)_{ab}^{\text{adj}}$ is a Wilson line in the adjoint representation connecting the point $(\mathbf{R}, 0)$ to (\mathbf{R}, t) . From Eq. (33) and (83) we may calculate the state normalization factor δZ_H :

$$\delta Z_{H(\lambda)} = \frac{\partial \delta E_{H(\lambda)}}{\partial E_H^{(0)}} = \frac{1}{6} \int_0^\infty dt t \langle 0 | g\mathbf{E}^a(\mathbf{R}, 0) \phi(0, t)_{ab}^{\text{adj}} g\mathbf{E}^b(\mathbf{R}, t) | 0 \rangle \times \langle H(\lambda) | \mathbf{r} e^{-i(E_H^{(0)} - h_O^{(0)})t} \mathbf{r} | H(\lambda) \rangle. \quad (84)$$

The leading color-octet contribution is given by the chromo-E1 operator (28). At second order in \mathbf{r} , there are four diagrams contributing to the transition amplitude, as shown in Fig. 5. The contribution of Fig. 5(a) corresponds to

$$\begin{aligned} & -^{(0)} \langle n'^1 S_0(\mathbf{P}') \gamma(\mathbf{k}, \sigma) | \int d^3 R \mathcal{L}_{\text{M1}}^{(0)} | n^3 S_1(\mathbf{0}, \lambda) \rangle \rangle_{\parallel}^{(2)} \\ & - \parallel^{(2)} \langle n'^1 S_0(\mathbf{P}') \gamma(\mathbf{k}, \sigma) | \int d^3 R \mathcal{L}_{\text{M1}}^{(0)} | n^3 S_1(\mathbf{0}, \lambda) \rangle \rangle^{(0)} \\ & = (2\pi)^3 \delta^3(\mathbf{P}' + \mathbf{k}) \bar{\mathcal{A}}^{(0)} [n^3 S_1(\mathbf{0}, \lambda) \rightarrow n'^1 S_0(-\mathbf{k}) \gamma(\mathbf{k}, \sigma)] \\ & \times c_F^{\text{em}} \frac{\delta_{nn'}}{3} \int_0^\infty dt t \langle 0 | g\mathbf{E}^a(\mathbf{R}, 0) \phi(0, t)_{ab}^{\text{adj}} g\mathbf{E}^b(\mathbf{R}, t) | 0 \rangle \\ & \times \langle n' S | \mathbf{r} e^{-i(E_n^{(0)} - h_O^{(0)})t} \mathbf{r} | n S \rangle. \end{aligned} \quad (85)$$

This diagram only contributes to M1 allowed transitions. The contribution of Fig. 5(b)

corresponds to

$$\begin{aligned}
& -^{(1)} \langle n'{}^1S_0(\mathbf{P}') \gamma(\mathbf{k}, \sigma) | \int d^3R \mathcal{L}_{M1}^{(0) \text{ octet}} | n^3S_1(\mathbf{0}, \lambda) \rangle^{(1)} \\
& = (2\pi)^3 \delta^3(\mathbf{P}' + \mathbf{k}) \bar{\mathcal{A}}^{(0)} [n^3S_1(\mathbf{0}, \lambda) \rightarrow n'{}^1S_0(-\mathbf{k}) \gamma(\mathbf{k}, \sigma)] \\
& \quad \times c_F^{\text{em}} \frac{i}{3} \int_0^\infty dt \frac{e^{i(E_n^{(0)} - E_{n'}^{(0)})t} - 1}{E_n^{(0)} - E_{n'}^{(0)}} \langle 0 | g \mathbf{E}^a(\mathbf{R}, 0) \phi(0, t)_{ab}^{\text{adj}} g \mathbf{E}^b(\mathbf{R}, t) | 0 \rangle \\
& \quad \times \langle n' S | \mathbf{r} e^{-i(E_n^{(0)} - h_O^{(0)})t} \mathbf{r} | n S \rangle, \tag{86}
\end{aligned}$$

$$\text{where } \mathcal{L}_{M1}^{(0) \text{ octet}} = \int d^3r \text{Tr} \left\{ \frac{1}{2m} \{ \mathbf{O}^\dagger, \boldsymbol{\sigma} \cdot e e_Q \mathbf{B}^{\text{em}} \} \mathbf{O} \right\}.$$

The sum of the contributions of Figs. 5(c) and 5(d) gives:

$$\begin{aligned}
& -^{(0)} \langle n'{}^1S_0(\mathbf{P}') \gamma(\mathbf{k}, \sigma) | \int d^3R \mathcal{L}_{M1}^{(0)} | n^3S_1(\mathbf{0}, \lambda) \rangle_{\perp}^{(2)} \\
& -_{\perp}^{(2)} \langle n'{}^1S_0(\mathbf{P}') \gamma(\mathbf{k}, \sigma) | \int d^3R \mathcal{L}_{M1}^{(0)} | n^3S_1(\mathbf{0}, \lambda) \rangle^{(0)} \\
& = (2\pi)^3 \delta^3(\mathbf{P}' + \mathbf{k}) \bar{\mathcal{A}}^{(0)} [n^3S_1(\mathbf{0}, \lambda) \rightarrow n'{}^1S_0(-\mathbf{k}) \gamma(\mathbf{k}, \sigma)] \\
& \quad \times i c_F^{\text{em}} \frac{1 - \delta_{nn'}}{3} \int_0^\infty dt \frac{1}{E_n^{(0)} - E_{n'}^{(0)}} \langle 0 | g \mathbf{E}^a(\mathbf{R}, 0) \phi(0, t)_{ab}^{\text{adj}} g \mathbf{E}^b(\mathbf{R}, t) | 0 \rangle \\
& \quad \times \langle n' S | \mathbf{r} \left(e^{-i(E_n^{(0)} - h_O^{(0)})t} - e^{-i(E_{n'}^{(0)} - h_O^{(0)})t} \right) \mathbf{r} | n S \rangle. \tag{87}
\end{aligned}$$

These diagrams only contribute to M1 hindered transitions.

Remarkably the sum of all octet contributions at relative order v^2 , i.e. Eqs. (85)-(87), vanishes. This relies, again, on the fact that the leading M1 operator behaves like the identity operator in coordinate space. Our cancellation proof, indeed, very much resembles the $V_S^{\frac{\sigma \cdot B}{m}}$ non-renormalization proof given in Sec. III B. The cancellation of all octet contributions at relative order v^2 is nothing more than a manifestation of the proper normalization of the quarkonium state when higher-order Fock-space components are taken into account.⁹

Finally, we note that, since the leading operator responsible for E1 transitions, given in Eq. (80), is not a unit operator in coordinate space, the above cancellation mechanism does not apply there. In the E1 case, when $\Lambda_{\text{QCD}} \sim mv^2$, we will, in general, have octet corrections of the same size as the leading relativistic ones. These have not been calculated so far, but may be of relevant phenomenological impact for electric-dipole transitions in weakly-coupled quarkonia.

⁹ On this see also Ref. [37].

V. FINAL FORMULAE INCORPORATING ALL $\mathcal{O}(v^2)$ CORRECTIONS

In this section, we sum all previously calculated contributions for transition amplitudes and give expressions for the widths.

A. $\mathcal{O}(v^2)$ S-wave transition amplitude

Summing Eqs. (35), (57), (58), (59), (61), (62), (63), (75), (77), (82), we obtain the M1 transition amplitude with $\mathcal{O}(v^2)$ corrections included:

$$\begin{aligned} \bar{\mathcal{A}} [n^3 S_1(\mathbf{0}, \lambda) \rightarrow n'{}^1 S_0(-\mathbf{k}) \gamma(\mathbf{k}, \sigma)] &= \delta_{nn'} (1 + \kappa_Q^{\text{em}}) \\ &+ (1 - \delta_{nn'}) \frac{1 + \kappa_Q^{\text{em}}}{m^2} \frac{\langle n' S | V^{\text{ss}}(\mathbf{r}) | n S \rangle}{E_n^{(0)} - E_{n'}^{(0)}} \\ &+ \langle n' S | \left[-\frac{1 + \kappa_Q^{\text{em}}}{24} k^2 \mathbf{r}^2 - \left(\frac{5}{3} + \kappa_Q^{\text{em}} \right) \frac{\mathbf{p}^2}{2m^2} + \frac{\kappa_Q^{\text{em}}}{6m} r V_S^{(0)\prime} \right] | n S \rangle. \end{aligned} \quad (88)$$

We have used $c_S^{\text{em}} = 1 + 2\kappa_Q^{\text{em}}$ and

$$i \frac{k}{m} \langle n' | \mathbf{r} \cdot \mathbf{p} | n \rangle = \langle n' | \left(-2 \frac{\mathbf{p}^2}{m^2} + \frac{r V_s^{(0)\prime}}{m} \right) | n \rangle + \mathcal{O}(v^4), \quad (89)$$

which holds for $(1 - \delta_{nn'}) k \approx (1 - \delta_{nn'}) (E_n^{(0)} - E_{n'}^{(0)}) \sim (1 - \delta_{nn'}) m v^2$ and $\delta_{nn'} k \sim \delta_{nn'} m v^4$, which we neglect. Terms of the type $\delta_{nn'} k$, which are beyond our accuracy, have been neglected also in Eq. (88).

B. S-wave transition widths

Inserting (88) into (12), we obtain the total transition width for magnetic dipole transitions of S -wave quarkonium up to order $k_\gamma^3 v^2/m^2$. We use the explicit one-loop value of κ_Q^{em} given in Eq. (7). In accordance to the power counting, we neglect order $\alpha_s^2(m)$ and order

$\alpha_s(m) v^2$ corrections. The final result reads

$$\Gamma_{n^3S_1 \rightarrow n^1S_0 \gamma} = \frac{4}{3} \alpha e_Q^2 \frac{k_\gamma^3}{m^2} \left[1 + C_F \frac{\alpha_s(m)}{\pi} - \frac{5}{3} \langle nS | \frac{\mathbf{p}^2}{m^2} | nS \rangle \right], \quad (90)$$

$$\begin{aligned} \Gamma_{n^3S_1 \rightarrow n'^1S_0 \gamma} &\stackrel{n \neq n'}{=} \frac{4}{3} \alpha e_Q^2 \frac{k_\gamma^3}{m^2} \left[\langle n'S | \left(-\frac{k_\gamma^2 \mathbf{r}^2}{24} - \frac{5}{6} \frac{\mathbf{p}^2}{m^2} \right) | nS \rangle \right. \\ &\quad \left. + \frac{1}{m^2} \frac{\langle n'S | V^{\text{ss}}(\mathbf{r}) | nS \rangle}{E_n^{(0)} - E_{n'}^{(0)}} \right]^2. \end{aligned} \quad (91)$$

For completeness, we also give the $n^1S_0 \rightarrow n'^3S_1 \gamma$ transition width, which is relevant only for hindered transitions:

$$\begin{aligned} \Gamma_{n^1S_0 \rightarrow n'^3S_1 \gamma} &\stackrel{n \neq n'}{=} 4 \alpha e_Q^2 \frac{k_\gamma^3}{m^2} \left[\langle n'S | \left(-\frac{k_\gamma^2 \mathbf{r}^2}{24} - \frac{5}{6} \frac{\mathbf{p}^2}{m^2} \right) | nS \rangle \right. \\ &\quad \left. - \frac{1}{m^2} \frac{\langle n'S | V^{\text{ss}}(\mathbf{r}) | nS \rangle}{E_n^{(0)} - E_{n'}^{(0)}} \right]^2. \end{aligned} \quad (92)$$

Equations (90)-(92) very much resemble those derived in [15] and subsequently used in most non-relativistic potential model calculations of the magnetic dipole transitions in quarkonium (see, for instance, the review in [21]). There are, however, some differences that we have already mentioned, but we would like to stress again.

(1) Equations (90)-(92) have a limited range of validity that the EFT framework clarifies. They are valid only in the weak-coupling limit, i.e. for quarkonia that fulfill the criterion $mv^2 \gtrsim \Lambda_{\text{QCD}}$. The lowest bottomonium states and the charmonium ground state may belong to quarkonia of this kind. As discussed in Sec. III D, in the strong-coupling regime, i.e. for higher-quarkonium excitations, at order $k_\gamma^3 v^2/m^2$ more terms will, in principle, arise.

(2) Equations (90)-(92) do not contain contributions from a scalar interaction (proportional to $-\langle n'S | V^{\text{scalar}} | m | nS \rangle$). This has been often used in potential models, but the analysis of Sec. III C has excluded such a contribution in pNRQCD.

(3) The analysis in Sec. III B has also excluded (to all orders) contributions to the quarkonium magnetic moment coming from the soft scale. This allows us to substitute κ_Q^{em} with the value inherited from NRQCD, which at one loop is $\kappa_Q^{\text{em}} = C_F \alpha_s / (2\pi)$. The renormalization scale of α_s is m .

(4) In Sec. IV B, it has been shown that color-octet contributions, not accessible to potential model analyses, cancel at order $k_\gamma^3 v^2/m^2$. This leads to the conclusion that in

the weak-coupling regime, at order $k_\gamma^3 v^2/m^2$, M1 transitions are completely accessible to perturbation theory. In particular, once the spin-spin potential is written at leading order in perturbation theory (which is sufficient here),

$$V^{\text{ss}}(\mathbf{r}) = \frac{8}{3} \pi C_F \alpha_s \delta^3(\mathbf{r}), \quad (93)$$

and Eqs. (90)-(92) are calculated for Coulomb wave functions, the transition rates will only depend on the strong-coupling constant.

C. P -wave transition widths

In this section, we consider only allowed M1 transitions between P -wave states. Since hindered P -wave transitions are unlikely to accommodate within a weakly-coupled picture. The calculation proceeds very much like the analogous one for S -wave states, so we will not present details here. Octet contributions again cancel by the same argument as given for S -wave transitions. At order $k_\gamma^3 v^2/m^2$, only two operators contribute to M1 allowed transitions: $\frac{1}{4m^3} \{S^\dagger, \boldsymbol{\sigma} \cdot ee_Q \mathbf{B}^{\text{em}}\} \nabla_r^2 S$ and $\frac{1}{4m^2} \frac{rV_S^{(0)'}(r)}{2} \{S^\dagger, \boldsymbol{\sigma} \cdot [\hat{\mathbf{r}} \times (\hat{\mathbf{r}} \times ee_Q \mathbf{B}^{\text{em}})]\} S$. Summing their contributions, at order $k_\gamma^3 v^2/m^2$, the final results read

$$\Gamma_{n^3 P_J \rightarrow n^1 P_1 \gamma} = \frac{4}{3} \alpha e_Q^2 \frac{k_\gamma^3}{m^2} \left[1 + C_F \frac{\alpha_s(m)}{\pi} - d_J \langle nP | \frac{\mathbf{p}^2}{m^2} | nP \rangle \right], \quad (94)$$

$$\Gamma_{n^1 P_1 \rightarrow n^3 P_J \gamma} = (2J+1) \frac{4}{9} \alpha e_Q^2 \frac{k_\gamma^3}{m^2} \left[1 + C_F \frac{\alpha_s(m)}{\pi} - d_J \langle nP | \frac{\mathbf{p}^2}{m^2} | nP \rangle \right], \quad (95)$$

where $d_0 = 1$, $d_1 = 2$ and $d_2 = 8/5$. We have made use of the virial theorem. Corrections induced by the operator $\frac{1}{4m^2} \frac{rV_S^{(0)'}(r)}{2} \{S^\dagger, \boldsymbol{\sigma} \cdot [\hat{\mathbf{r}} \times (\hat{\mathbf{r}} \times ee_Q \mathbf{B}^{\text{em}})]\} S$ vanish for $J = 0$ states.

Combining Eq. (90) with Eqs. (94) and (95), we obtain that, at leading order, the following relations hold:

$$\frac{3 \Gamma_{n^1 P_1 \rightarrow n^3 P_0 \gamma} - \Gamma_{n^3 S_1 \rightarrow n^1 S_0 \gamma}}{\Gamma_{n^3 P_2 \rightarrow n^1 P_1 \gamma} - \Gamma_{n^3 S_1 \rightarrow n^1 S_0 \gamma}} = 10, \quad \frac{\Gamma_{n^3 S_1 \rightarrow n^1 S_0 \gamma} - \Gamma_{n^1 P_1 \rightarrow n^3 P_1 \gamma}}{\Gamma_{n^3 P_2 \rightarrow n^1 P_1 \gamma} - \Gamma_{n^3 S_1 \rightarrow n^1 S_0 \gamma}} = 5, \quad (96)$$

which follow from $\langle nS | \frac{\mathbf{p}^2}{m^2} | nS \rangle = \langle nP | \frac{\mathbf{p}^2}{m^2} | nP \rangle = -\frac{E_n^{(0)}}{m}$.¹⁰

¹⁰ So far, we have labeled P -wave states with their principal quantum number n . In the next section, we will follow the usual convention for which a $\chi(1P)$ state is a $n = 2$, $L = 1$ state.

VI. APPLICATIONS

We have remarked that Eqs. (90)-(92), (94) and (95) are valid only for weakly-coupled quarkonia. It is generally believed that the lowest-lying $b\bar{b}$ states, $\Upsilon(1S)$ and η_b , are in the weak-coupling regime. The situation for $\chi_b(1P)$, $h_b(1P)$, $\Upsilon(2S)$ and $\eta_b(2S)$ is more controversial as it is for the lowest-lying $c\bar{c}$ states. We will assume that also these states are weakly coupled and see whether the comparison between our predictions and the experimental data supports this assumption or not. As for the $n = 2$ charmonium states, it is undoubtedly inappropriate to consider them as weakly-coupled systems. A further complication of the $\psi(2S)$ and $\eta_c(2S)$ states is that they lie too close to the open charm threshold, so that threshold effects should be included in a proper EFT treatment. We will not consider them in our analysis. In the following, we shall apply Eqs. (90)-(92) to $J/\psi \rightarrow \eta_c \gamma$, $\Upsilon(1S) \rightarrow \eta_b \gamma$, $\Upsilon(2S) \rightarrow \eta_b(2S) \gamma$, $\Upsilon(2S) \rightarrow \eta_b \gamma$ and $\eta_b(2S) \rightarrow \Upsilon(1S) \gamma$, and Eqs. (94) and (95) to $h_b(1P) \rightarrow \chi_{b0,1}(1P) \gamma$ and $\chi_{b2}(1P) \rightarrow h_b(1P) \gamma$.

A. $J/\psi \rightarrow \eta_c \gamma$

In potential models, the transition $J/\psi \rightarrow \eta_c \gamma$ has been often considered problematic to accommodate because its leading-order width is about 2.83 keV (for $m_c = M_{J/\psi}/2 = 1548$ MeV), far away from the experimental value of (1.18 ± 0.36) keV [38].

Since we assume that the charmonium ground state is a weakly-coupled quarkonium, Eq. (90) provides the transition width up to order $k_\gamma^3 v_c^2/m^2$. We may conveniently rewrite it as

$$\begin{aligned} \Gamma_{J/\psi \rightarrow \eta_c \gamma} &= \frac{16}{3} \alpha e_c^2 \frac{k_\gamma^3}{M_{J/\psi}^2} \left[1 + C_F \frac{\alpha_s(M_{J/\psi}/2)}{\pi} + \frac{2}{3} \frac{\langle 1S | 3V_S^{(0)} - rV_S^{(0)'} | 1S \rangle}{M_{J/\psi}} \right] \\ &= \frac{16}{3} \alpha e_c^2 \frac{k_\gamma^3}{M_{J/\psi}^2} \left[1 + C_F \frac{\alpha_s(M_{J/\psi}/2)}{\pi} - \frac{2}{3} (C_F \alpha_s(p_{J/\psi}))^2 \right], \end{aligned} \quad (97)$$

where in the first line we have reexpressed the charm mass in terms of the J/ψ mass,

$$M_{J/\psi} = 2m_c + \langle 1S | \frac{\mathbf{p}^2}{m_c} + V_S^{(0)}(r) | 1S \rangle,$$

and made use of the virial theorem to get rid of the kinetic energy. We have made explicit in Eq. (97) that the normalization scale for the α_s inherited from κ_c^{em} is the charm mass

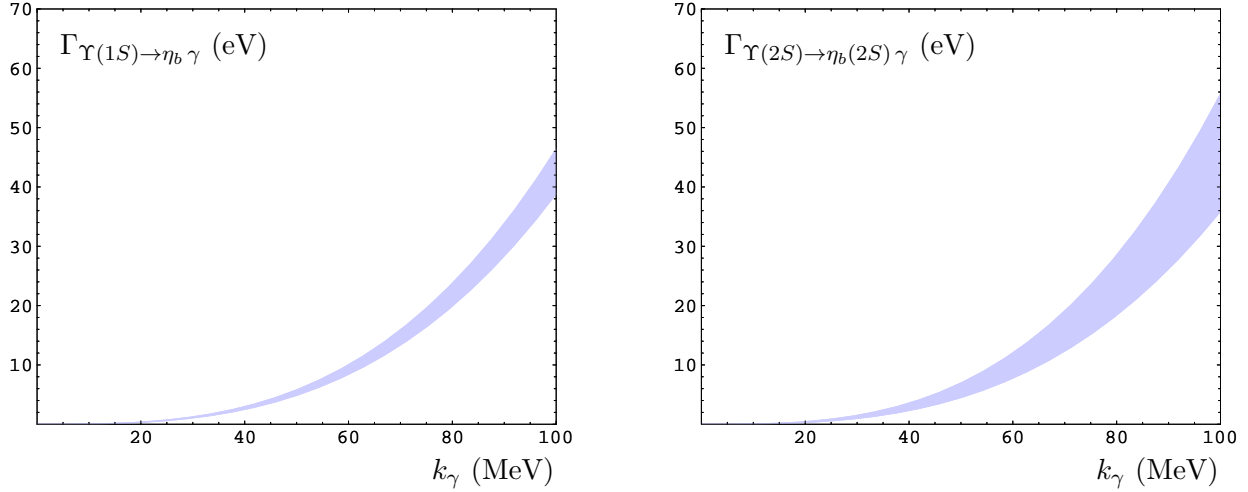


FIG. 6: $\Gamma_{\Upsilon(1S) \rightarrow \eta_b \gamma}$ and $\Gamma_{\Upsilon(2S) \rightarrow \eta_b(2S) \gamma}$ as a function of the photon energy.

($\alpha_s(M_{J/\psi}/2) \approx 0.35$), and for the α_s , which comes from the Coulomb potential, is the typical momentum transfer $p_{J/\psi} \approx m C_F \alpha_s(p_{J/\psi})/2 \approx 0.8$ GeV. Numerically we obtain:

$$\Gamma_{J/\psi \rightarrow \eta_c \gamma} = (1.5 \pm 1.0) \text{ keV.} \quad (98)$$

The uncertainty has been estimated by assuming the next corrections to be suppressed by a factor $\alpha_s^3(p_{J/\psi})$ with respect to the transition width in the non-relativistic limit.

Some comments are in order. First, we note that the uncertainty in (98) is large. In our view, it fully accounts for the large uncertainty coming from higher-order relativistic corrections, which may be large if we consider that those of order $k_\gamma^3 v_c^2/m^2$ have reduced the leading-order result by about 50%, and for the uncertainties in the normalization scales of the strong-coupling constant. Both uncertainties may be only reduced by higher-order calculations.

Despite the uncertainties, the value given in Eq. (98) is perfectly consistent with the experimental one. This means that assuming the ground-state charmonium to be a weakly-coupled system leads to relativistic corrections to the transition width of the right sign and size. This is not trivial. If we look at the first expression after the equality in Eq. (97), we may notice that $3V_S^{(0)} - rV_S^{(0) \prime}$ is negative in the case of a Coulomb potential (i.e. it lowers the transition width), but positive in the case of a confining linear potential (i.e. it increases the transition width). This may explain some of the difficulties met by potential models in reproducing $\Gamma_{J/\psi \rightarrow \eta_c \gamma}$. In any rate, it should be remembered that Eq. (97) is not the correct expression to be used in the strong-coupling regime.

B. $\Upsilon(1S) \rightarrow \eta_b \gamma, \Upsilon(2S) \rightarrow \eta_b(2S) \gamma$

Allowed M1 transitions in the bottomonium system that may be treated by the weak-coupling formula (90) are $\Upsilon(1S) \rightarrow \eta_b \gamma$ and, perhaps, $\Upsilon(2S) \rightarrow \eta_b(2S) \gamma$. We have

$$\Gamma_{\Upsilon(1S) \rightarrow \eta_b \gamma} = \frac{16}{3} \alpha e_b^2 \frac{k_\gamma^3}{M_{\Upsilon(1S)}^2} \left[1 + C_F \frac{\alpha_s(M_{\Upsilon(1S)}/2)}{\pi} - \frac{2}{3} (C_F \alpha_s(p_{\Upsilon(1S)}))^2 \right], \quad (99)$$

$$\Gamma_{\Upsilon(2S) \rightarrow \eta_b(2S) \gamma} = \frac{16}{3} \alpha e_b^2 \frac{k_\gamma^3}{M_{\Upsilon(1S)}^2} \left[1 + C_F \frac{\alpha_s(M_{\Upsilon(1S)}/2)}{\pi} - \left(\frac{C_F \alpha_s(p_{\Upsilon(1S)})}{2} \right)^2 - \frac{5}{3} \left(\frac{C_F \alpha_s(p_{\Upsilon(2S)})}{4} \right)^2 \right], \quad (100)$$

where we have expressed the b mass in terms of the $\Upsilon(1S)$ mass. We have made explicit that the renormalization scale for the α_s , inherited from κ_b^{em} , is the bottom mass ($\alpha_s(M_{\Upsilon(1S)}/2) \approx 0.22$), while for the α_s , which comes from the Coulomb potential in the $\Upsilon(1S)$ system, is the typical momentum transfer $p_{\Upsilon(1S)} \approx m C_F \alpha_s(p_{\Upsilon(1S)})/2 \approx 1.2$ GeV, and for the α_s , which comes from the Coulomb potential in the $\Upsilon(2S)$ system, is the typical momentum transfer $p_{\Upsilon(2S)} \approx m C_F \alpha_s(p_{\Upsilon(2S)})/4 \approx 0.9$ GeV.

Since the η_b has not been discovered yet, in Fig. 6 we show $\Gamma_{\Upsilon(1S) \rightarrow \eta_b \gamma}$ and $\Gamma_{\Upsilon(2S) \rightarrow \eta_b(2S) \gamma}$ as a function of k_γ . The bands stand for the uncertainties calculated as the product of the transition widths in the non-relativistic limit by $\alpha_s^3(p_{\Upsilon(1S)})$ and $\alpha_s^3(p_{\Upsilon(2S)})$ respectively. If we use the value of the η_b mass given in [39], i.e. $k_\gamma = 39 \pm 13$ MeV, we have

$$\Gamma_{\Upsilon(1S) \rightarrow \eta_b \gamma} = (3.6 \pm 2.9) \text{ eV}, \quad (101)$$

which corresponds to a branching fraction of $(6.8 \pm 5.5) \times 10^{-5}$.

C. $\Upsilon(2S) \rightarrow \eta_b \gamma, \eta_b(2S) \rightarrow \Upsilon(1S) \gamma$

For hindered M1 transitions, Eqs. (91) and (92) only provide the leading-order expressions. We consider, here, $\Upsilon(2S) \rightarrow \eta_b \gamma$ and $\eta_b(2S) \rightarrow \Upsilon(1S) \gamma$ transition widths that we write as

$$\Gamma_{\Upsilon(2S) \rightarrow \eta_b \gamma} = \frac{16}{3} \alpha e_b^2 \frac{k_\gamma^3}{M_{\Upsilon(1S)}^2} \left[\frac{31\sqrt{2}}{81} (C_F \alpha_s)^2 + \frac{1024\sqrt{2}}{729} \frac{k_\gamma^2}{(M_{\Upsilon(1S)} C_F \alpha_s)^2} \right]^2, \quad (102)$$

$$\Gamma_{\eta_b(2S) \rightarrow \Upsilon(1S) \gamma} = 16 \alpha e_b^2 \frac{k_\gamma^3}{M_{\Upsilon(1S)}^2} \left[-\frac{41\sqrt{2}}{81} (C_F \alpha_s)^2 + \frac{1024\sqrt{2}}{729} \frac{k_\gamma^2}{(M_{\Upsilon(1S)} C_F \alpha_s)^2} \right]^2. \quad (103)$$

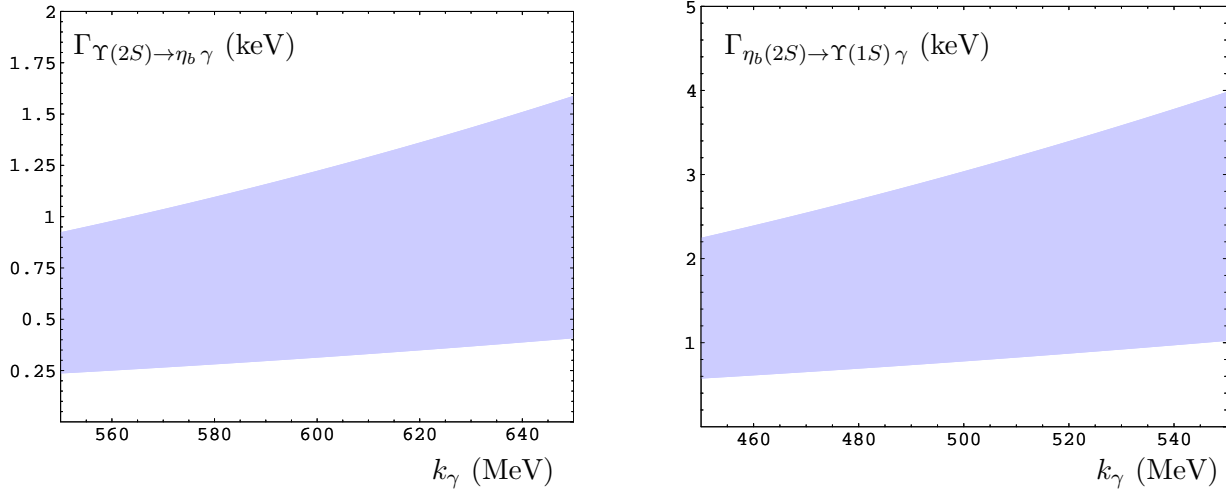


FIG. 7: $\Gamma_{\Upsilon(2S) \rightarrow \eta_b \gamma}$ and $\Gamma_{\eta_b(2S) \rightarrow \Upsilon(1S) \gamma}$ as a function of the photon energy.

Since terms arising from the $1S$ and $2S$ system mix, it is difficult to assign a natural normalization scale to α_s appearing in Eqs. (102) and (103) without doing a higher-order calculation. In Fig. 7, we show a plot of $\Gamma_{\Upsilon(2S) \rightarrow \eta_b \gamma}$ and $\Gamma_{\eta_b(2S) \rightarrow \Upsilon(1S) \gamma}$ as a function of k_γ . The scale of α_s appearing in Eqs. (102) and (103) has been arbitrarily fixed to 1 GeV. The bands stand for the uncertainties calculated as the products of the transition widths by $\alpha_s(p_{\Upsilon(2S)})$.

CLEO III recently set the 90% upper limit for the branching fraction of $\Upsilon(2S) \rightarrow \eta_b \gamma$ to be 0.5×10^{-3} [40]. The values plotted in Fig. 7 are about a factor 10 above the limit.¹¹ Despite the fact that our calculation is just a leading order one and, therefore, potentially affected by large uncertainties, it is not obvious that perturbation theory may accommodate for such a large discrepancy. In case, this may hint to a strongly-coupled interpretation of the bottomonium $2S$ states.¹²

D. $h_b(1P) \rightarrow \chi_{b0,1}(1P) \gamma, \chi_{b2}(1P) \rightarrow h_b(1P) \gamma$

P -wave M1 transitions that may be possibly described by pNRQCD in the weak-coupling regime are M1 allowed transitions between $n = 2$ bottomonium states. Proceeding like in

¹¹ Large contributions stem from the spin-spin potential term. If instead of using $E_2^{(0)} - E_1^{(0)}$ in this term, we use the physical mass difference, the decay width reduces by about a factor one half.

¹² A conclusion of this kind has been reached in [41] from the study of $\Upsilon(2S) \rightarrow X \gamma$ radiative decays. On the other hand, the masses of the $n = 2$ bottomonium states seem easier to accommodate within a weakly-coupled picture [42, 43, 44].

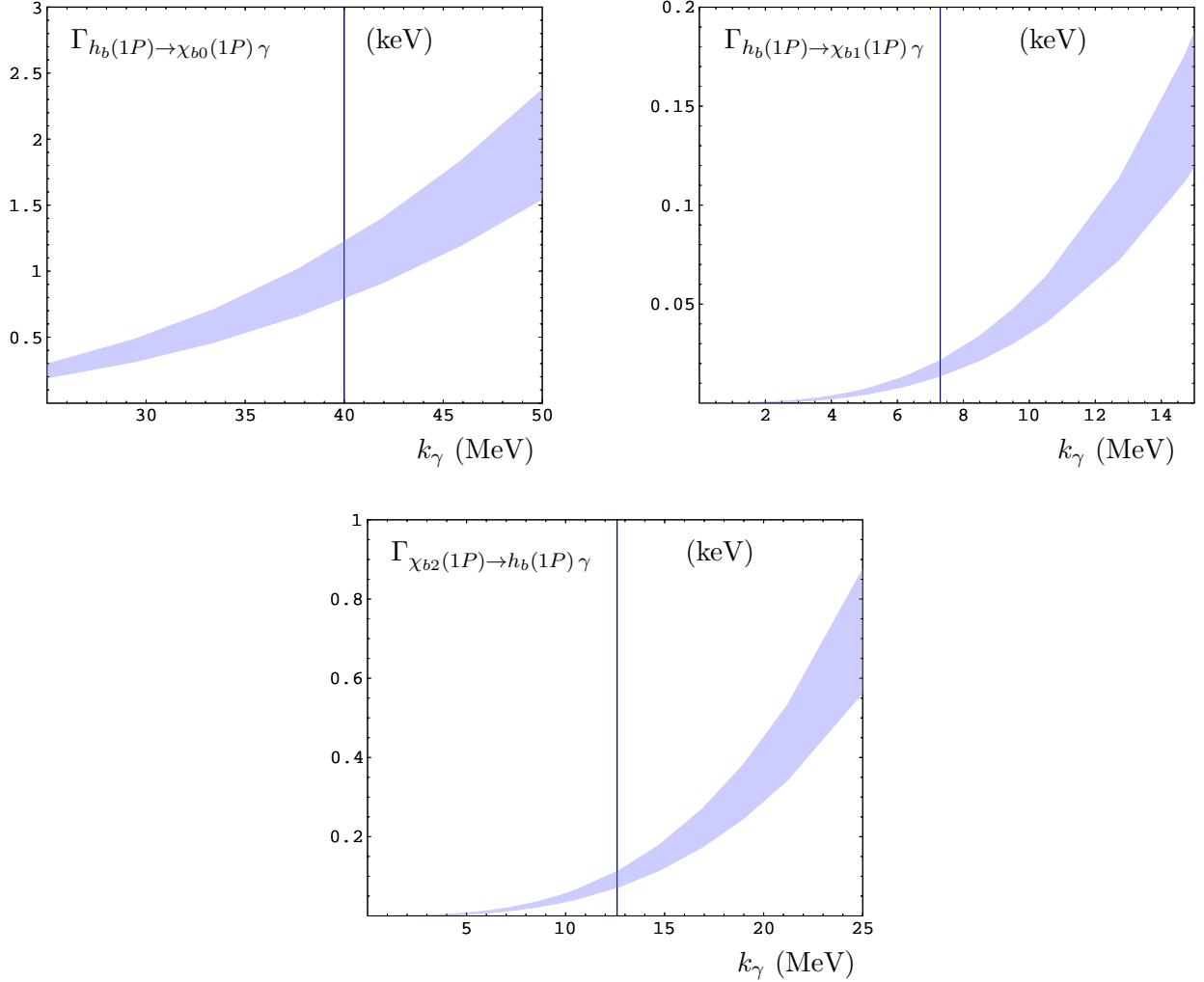


FIG. 8: $\Gamma_{hb(1P) \rightarrow \chi_{b0}(1P)\gamma}$, $\Gamma_{hb(1P) \rightarrow \chi_{b1}(1P)\gamma}$ and $\Gamma_{\chi_{b2}(1P) \rightarrow hb(1P)\gamma}$ as a function of the photon energy. The vertical lines correspond to the centre-of-gravity mass of the $\chi_{bJ}(1P)$ states, which is about 9900 MeV. This is believed to be a rather accurate estimate of the $hb(1P)$ mass. For this value of the $hb(1P)$ mass, we obtain $\Gamma_{hb(1P) \rightarrow \chi_{b0}(1P)\gamma} = 1 \pm 0.2$ keV, $\Gamma_{hb(1P) \rightarrow \chi_{b1}(1P)\gamma} = 17 \pm 4$ eV and $\Gamma_{\chi_{b2}(1P) \rightarrow hb(1P)\gamma} = 90 \pm 20$ eV.

Sec. VI B, we obtain

$$\begin{aligned} \Gamma_{hb(1P) \rightarrow \chi_{b0}(1P)\gamma} = \frac{16}{9} \alpha e_b^2 \frac{k_\gamma^3}{M_{\Upsilon(1S)}^2} & \left[1 + C_F \frac{\alpha_s(M_{\Upsilon(1S)}/2)}{\pi} - \left(\frac{C_F \alpha_s(p_{\Upsilon(1S)})}{2} \right)^2 \right. \\ & \left. - \left(\frac{C_F \alpha_s(p_{\chi_{b0}(1P)})}{4} \right)^2 \right], \end{aligned} \quad (104)$$

$$\Gamma_{h_b(1P) \rightarrow \chi_{b1}(1P) \gamma} = \frac{16}{3} \alpha e_b^2 \frac{k_\gamma^3}{M_{\Upsilon(1S)}^2} \left[1 + C_F \frac{\alpha_s(M_{\Upsilon(1S)}/2)}{\pi} - \left(\frac{C_F \alpha_s(p_{\Upsilon(1S)})}{2} \right)^2 - 2 \left(\frac{C_F \alpha_s(p_{\chi_b(1P)})}{4} \right)^2 \right], \quad (105)$$

and

$$\Gamma_{\chi_{b2}(1P) \rightarrow h_b(1P) \gamma} = \frac{16}{3} \alpha e_b^2 \frac{k_\gamma^3}{M_{\Upsilon(1S)}^2} \left[1 + C_F \frac{\alpha_s(M_{\Upsilon(1S)}/2)}{\pi} - \left(\frac{C_F \alpha_s(p_{\Upsilon(1S)})}{2} \right)^2 - \frac{8}{5} \left(\frac{C_F \alpha_s(p_{\chi_b(1P)})}{4} \right)^2 \right]. \quad (106)$$

Since the $h_b(1P)$ has not been discovered yet, in Fig. 8 we show $\Gamma_{h_b(1P) \rightarrow \chi_{b0}(1P) \gamma}$, $\Gamma_{h_b(1P) \rightarrow \chi_{b1}(1P) \gamma}$ and $\Gamma_{\chi_{b2}(1P) \rightarrow h_b(1P) \gamma}$ as a function of k_γ . We assume $p_{\Upsilon(\chi_b(1P))} \approx p_{\Upsilon(\Upsilon(2S))} \approx 0.9$ GeV. The bands stand for the uncertainties calculated as in Sec. VI B. Specific predictions of pNRQCD in the weak-coupling regime are also Eqs. (96) for $n = 2$.

VII. CONCLUSION AND OUTLOOK

The paper constitutes a through study of magnetic dipole transitions in the framework of non-relativistic EFTs of QCD and, in particular, of pNRQCD. The matching of the magnetic dipole operators at order $1/m$ and $1/m^2$ of pNRQCD has been performed to all orders in α_s . The matching at order $1/m^3$ has been carried out at leading order in the weak-coupling regime. Relativistic corrections to the transition widths have been included in a systematic fashion. Having achieved this, we could answer the questions raised in the introduction. (i) The contribution to the quarkonium anomalous magnetic moment coming from the soft scale vanishes to all orders. (ii) There are no contributions to the magnetic dipole operators of the type induced by a scalar potential. (iii) In the weak-coupling regime, non-perturbative corrections due to color-octet contributions vanish at leading order.

Our final formulae (90)-(92) are the same as in [15], once cleaned of the scalar potential and once the one-loop expression of the quarkonium anomalous magnetic moment has been used. They are valid only for quarkonia that fulfill the condition $mv^2 \gtrsim \Lambda_{\text{QCD}}$, i.e. only for the lowest-lying resonances. The application of Eq. (90) to the transition $J/\psi \rightarrow \eta_c \gamma$ shows that a weak-coupling treatment of the charmonium ground state is consistent with the data. We also provide a prediction for the analogous transition in the bottomonium case. Equations (94) and (95) are, to our knowledge, new.

Higher resonances that obey the condition $\Lambda_{\text{QCD}} \sim mv$ are described by pNRQCD in the strong-coupling regime. In this case, more operators, arising from the $1/m^3$ matching, are likely needed.

This work provides a first step towards a complete treatment of quarkonium radiative transitions in the framework of non-relativistic EFTs of QCD. Some of the next steps are obvious and we shall conclude by commenting on some of them.

(1) To describe M1 transitions for higher resonances the completion of the non-perturbative matching of the relevant pNRQCD operators at order $1/m^3$ will be needed. The matching coefficients will be Wilson-loop amplitudes similar to those that describe the non-perturbative potential at order $1/m^2$ [30]. This calculation, combined with a lattice simulation of the Wilson-loop amplitudes, may provide a rigorous QCD derivation for all quarkonium M1 transitions below threshold.

(2) M1 hindered transitions of the type $\Upsilon(3S) \rightarrow \eta_b \gamma$ have been also studied at CLEO III [40]. They involve emitted photons whose momentum is comparable with the typical momentum-transfer in the bound state. Then one cannot rely anymore on the multipole expansion of the external electromagnetic fields. In this case, however, one may exploit the hierarchy $p_{\eta_b} \gg \Lambda_{\text{QCD}} \gtrsim p_{\Upsilon(3S)}$. To our knowledge, this situation has not been analyzed so far.

(3) Electric dipole transitions have been mentioned only superficially in the paper. The pNRQCD operators, relevant for E1 transitions beyond leading order, have not been given. In the weak-coupling regime, octet contributions may be important and can be worked out along the lines discussed here. However, most of E1 transitions may need to be treated in a strong-coupling framework.

Acknowledgments

We thank Joan Soto for discussions and Tom Ferguson for correspondence. A.V. acknowledges the financial support obtained inside the Italian MIUR program “incentivazione alla mobilità di studiosi stranieri e italiani residenti all'estero”. A.V. and Y.J. were funded by Marie Curie Reintegration Grant contract MERG-CT-2004-510967.

APPENDIX A: FINAL-STATE RECOIL EFFECTS

We present here two alternative derivations of the final-state recoil effects calculated in Sec. IV A 2.

1. Recoil effects from Lorentz boosts

The effect on the quarkonium state of higher-order potentials that depend on the centre-of-mass momentum \mathbf{P} may also be calculated by boosting the quarkonium state at rest by $-\mathbf{P}/M_H \approx -\mathbf{P}/(2m)$ (i.e. minus the recoiling velocity). The importance of boost effects on the final-state quarkonium was first pointed out by Grotch and Sebastian in [12]. In our language, their argument goes as follows.

The Lorentz-boost generators \mathbf{K} of pNRQCD may be read from [28]. The leading spin-flipping contribution to \mathbf{K} is given by

$$\delta\mathbf{K} = \int d^3R \int d^3r \frac{i}{4m} \text{Tr} \{ [\mathbf{S}^\dagger, \boldsymbol{\sigma} \times \boldsymbol{\nabla}_r] \mathbf{S} \} . \quad (\text{A1})$$

It boosts the field \mathbf{S}^\dagger by an amount

$$\delta\mathbf{S}^\dagger = -i \left[-\frac{\mathbf{P}}{2m} \cdot \delta\mathbf{K}, \mathbf{S}^\dagger \right] = \epsilon_{ijk} \frac{\mathbf{P}^i}{8m^2} \{ \boldsymbol{\nabla}_r^k \mathbf{S}^\dagger, \boldsymbol{\sigma}^j \} . \quad (\text{A2})$$

Substituting (A2) into

$$\int d^3R \int d^3r e^{i\mathbf{P} \cdot \mathbf{R}} \text{Tr} \{ \Phi_{H(\lambda)}(\mathbf{r}) \delta\mathbf{S}^\dagger(\mathbf{r}, \mathbf{R}) |0\rangle \} , \quad (\text{A3})$$

we obtain Eq. (79).

2. Covariant formulation

Final-state recoil effects are automatically included in any Lorentz covariant definition of the wave function, like that one provided by the Bethe–Salpeter equation [45]. In momentum space, the Bethe–Salpeter wave function has the following spin structure:

$$\Phi_H^{\text{BS}} \propto \frac{P/2 + \not{p} + m}{2m} \frac{1 + \not{u}}{2} \mathcal{G}_H \frac{P/2 - \not{p} - m}{2m} , \quad (\text{A4})$$

where, at the order we are interested in, $P^\mu \approx (2m, \mathbf{P})$ is the centre-of-mass momentum, $p^\mu \approx (0, \mathbf{p})$ is the quark-antiquark relative momentum, $u^\mu \approx (1, \mathbf{P}/(2m))$, $\mathcal{G}_{n^1S_0} = \gamma^5$ and $\mathcal{G}_{n^3S_1(\lambda)} = \not{\phi}_{n^3S_1}(\lambda)$, with $u \cdot e_{n^3S_1}(\lambda) = 0$.

Expanding Φ_H^{BS} in \mathbf{P} and \mathbf{p} and keeping the upper-right $2 \otimes 2$ block we obtain

$$\Phi_{n^1 S_0}^{\text{BS}} \propto 1 - \frac{i}{4m^2} \mathbf{P} \cdot (\boldsymbol{\sigma} \times \mathbf{p}) + \dots, \quad (\text{A5})$$

$$\Phi_{n^3 S_1(\lambda)}^{\text{BS}} \propto \boldsymbol{\sigma} \cdot \mathbf{e} - \frac{i}{4m^2} \mathbf{P} \cdot (\mathbf{e}_{n^3 S_1}(\lambda) \times \mathbf{p}) + \dots. \quad (\text{A6})$$

The first terms in the equations give the spin structures of Eqs. (20) and (21), the second ones provide $\langle 0 | S(\mathbf{r}, \mathbf{R}) | n^1 S_0(\mathbf{P}) \rangle^{(1)}$ and $\langle 0 | S(\mathbf{r}, \mathbf{R}) | n^3 S_1(\mathbf{P}, \lambda) \rangle^{(1)}$ respectively, where $|H(\mathbf{P}, \lambda)\rangle^{(1)}$ has been given in Eq. (79).

APPENDIX B: GAUGE INVARIANCE

In the main text, we have employed an explicitly gauge-invariant formulation. In the literature, however, this has never been the case. As a consequence, partial results may differ. In this appendix, in order to make contact with the existing literature, we recalculate M1 transitions in a formulation of pNRQCD where $U(1)_{\text{em}}$ gauge invariance is not manifest at the Lagrangian level. This means that we shall express the pNRQCD Lagrangian in terms of the fields S' and O' defined in Eq. (44). Of course, the final, total results are identical in the two formulations.

If the calculation of M1 transitions in pNRQCD is performed in terms of the field S' , two are the main changes.

(1) The first change concerns $1/m^2$ operators. As discussed in Sec. III C, these may be obtained by projecting (71) onto a two-quark state. If the projection is performed on (43) and (44), we obtain the operator¹³

$$-\frac{1}{4m^2} \frac{rV_S^{(0)'}(r)}{2} \{S'^\dagger, \boldsymbol{\sigma} \cdot [\hat{\mathbf{r}} \times (\hat{\mathbf{r}} \cdot \boldsymbol{\nabla} ee_Q \mathbf{A}^{\text{em}})]\} S'. \quad (\text{B1})$$

It induces the following correction to S -wave transition widths

$$\bar{\mathcal{A}} [n^3 S_1(\mathbf{0}, \lambda) \rightarrow n'^1 S_0(-\mathbf{k}) \gamma(\mathbf{k}, \sigma)] = -\frac{1}{12m} \langle n' S | rV_S^{(0)'} | n S \rangle, \quad (\text{B2})$$

which differs by a factor $1/2$ from Eq. (75).

¹³ The leading operator in the multipole expansion, proportional to $\boldsymbol{\sigma} \cdot \hat{\mathbf{r}} \times ee_Q \mathbf{A}^{\text{em}}$, does not contribute to M1 transitions.

(2) The second change concerns final-state recoil effects. These have been calculated in a gauge invariant formulation in Sec. IV A 2. In terms of the fields S' , E1 transitions are mediated by (to be compared with Eq. (80))

$$-2i \int d^3r \text{Tr} \left\{ S'^\dagger \frac{ee_Q \mathbf{A}^{\text{em}} \cdot \nabla_r}{m} S' \right\}. \quad (\text{B3})$$

The correction to S -wave transition widths induced by (B3) on a recoiling final state is

$$\bar{\mathcal{A}} [n^3 S_1(\mathbf{0}, \lambda) \rightarrow n'^1 S_0(-\mathbf{k}) \gamma(\mathbf{k}, \sigma)] = -\langle n' S | \frac{\mathbf{p}^2}{6m^2} | n S \rangle. \quad (\text{B4})$$

This is exactly the result first derived in [12]. Note that, at order v^2 , Eq. (B4) also contributes to M1 allowed transitions, while Eq. (82) only contributes to M1 hindered transitions.

Summing Eqs. (B2) and (B4) we obtain

$$\langle n' S | \left(-\frac{1}{12m} r V_S^{(0)\prime} - \frac{\mathbf{p}^2}{6m^2} \right) | n S \rangle.$$

Summing Eqs. (75) and (82) we obtain

$$\langle n' S | \left[-\frac{1}{6m} r V_S^{(0)\prime} + \frac{k}{4m} \left(\delta_{n'n} + \frac{i}{3} \mathbf{r} \cdot \mathbf{p} \right) \right] | n S \rangle.$$

By using Eq. (89) and $\delta_{n'n} k \sim \delta_{n'n} m v^4$, one can easily see that the two expressions are equal at order v^2 . It is straightforward to perform the same check also in the case of P -wave transitions.

- [1] W. E. Caswell and G. P. Lepage, Phys. Lett. B **167**, 437 (1986).
- [2] G. T. Bodwin, E. Braaten and G. P. Lepage, Phys. Rev. D **51**, 1125 (1995) [Erratum-ibid. D **55**, 5853 (1997)] [hep-ph/9407339].
- [3] A. Pineda and J. Soto, Nucl. Phys. Proc. Suppl. **64**, 428 (1998) [arXiv:hep-ph/9707481].
- [4] N. Brambilla, A. Pineda, J. Soto and A. Vairo, Nucl. Phys. B **566**, 275 (2000) [arXiv:hep-ph/9907240].
- [5] N. Brambilla, A. Pineda, J. Soto and A. Vairo, Rev. Mod. Phys. **77**, 1423 (2005) [arXiv:hep-ph/0410047].
- [6] G. Feinberg and J. Sucher, Phys. Rev. Lett. **35**, 1740 (1975).
- [7] J. Sucher, Rept. Prog. Phys. **41**, 1781 (1978).

[8] E. Eichten, K. Gottfried, T. Kinoshita, K. D. Lane and T. M. Yan, Phys. Rev. D **17**, 3090 (1978) [Erratum-ibid. D **21**, 313 (1980)]; E. Eichten, K. Gottfried, T. Kinoshita, K. D. Lane and T. M. Yan, Phys. Rev. D **21**, 203 (1980).

[9] J. S. Kang and J. Sucher, Phys. Rev. D **18**, 2698 (1978).

[10] K. J. Sebastian, Phys. Rev. D **26**, 2295 (1982).

[11] G. Karl, S. Meshkov and J. L. Rosner, Phys. Rev. Lett. **45**, 215 (1980).

[12] H. Grotch and K. J. Sebastian, Phys. Rev. D **25**, 2944 (1982).

[13] P. Moxhay and J. L. Rosner, Phys. Rev. D **28**, 1132 (1983).

[14] R. McClary and N. Byers, Phys. Rev. D **28**, 1692 (1983); V. Zambetakis and N. Byers, Phys. Rev. D **28**, 2908 (1983).

[15] H. Grotch, D. A. Owen and K. J. Sebastian, Phys. Rev. D **30**, 1924 (1984).

[16] Fayyazuddin and O. H. Mobarek, Phys. Rev. D **48**, 1220 (1993).

[17] T. A. Lahde, Nucl. Phys. A **714**, 183 (2003) [arXiv:hep-ph/0208110].

[18] D. Ebert, R. N. Faustov and V. O. Galkin, Phys. Rev. D **67**, 014027 (2003) [arXiv:hep-ph/0210381].

[19] T. Barnes, S. Godfrey and E. S. Swanson, Phys. Rev. D **72**, 054026 (2005) [arXiv:hep-ph/0505002].

[20] A. Y. Khodjamirian, Phys. Lett. B **90**, 460 (1980).

[21] N. Brambilla *et al.*, CERN-2005-005, (CERN, Geneva, 2005) [arXiv:hep-ph/0412158].

[22] A. Le Yaouanc, L. Oliver, O. Pene and J. C. Raynal, “Hadron Transitions In The Quark Model”, ed. Gordon and Breach (New York, 1988), 311p.

[23] A. V. Manohar, Phys. Rev. D **56**, 230 (1997) [hep-ph/9701294].

[24] M. Beneke, arXiv:hep-ph/9911490.

[25] N. Brambilla, Y. Sumino and A. Vairo, Phys. Rev. D **65**, 034001 (2002) [arXiv:hep-ph/0108084].

[26] D. Gromes, Z. Phys. C **26**, 401 (1984).

[27] N. Brambilla, D. Gromes and A. Vairo, Phys. Rev. D **64**, 076010 (2001) [arXiv:hep-ph/0104068].

[28] N. Brambilla, D. Gromes and A. Vairo, Phys. Lett. B **576**, 314 (2003) [hep-ph/0306107].

[29] E. Eichten and F. Feinberg, Phys. Rev. D **23**, 2724 (1981).

[30] A. Pineda and A. Vairo, Phys. Rev. D **63**, 054007 (2001) [Erratum-ibid. D **64**, 039902 (2001)]

[arXiv:hep-ph/0009145].

- [31] X. Zhang, K. J. Sebastian and H. Grotch, Phys. Rev. D **44**, 1606 (1991).
- [32] N. Brambilla, A. Pineda, J. Soto and A. Vairo, Phys. Rev. D **63**, 014023 (2001) [arXiv:hep-ph/0002250].
- [33] N. Brambilla, A. Pineda, J. Soto and A. Vairo, Phys. Lett. B **580**, 60 (2004) [arXiv:hep-ph/0307159].
- [34] N. Brambilla, D. Eiras, A. Pineda, J. Soto and A. Vairo, Phys. Rev. Lett. **88**, 012003 (2002) [arXiv:hep-ph/0109130].
- [35] N. Brambilla, D. Eiras, A. Pineda, J. Soto and A. Vairo, Phys. Rev. D **67**, 034018 (2003) [arXiv:hep-ph/0208019].
- [36] N. Brambilla, A. Pineda, J. Soto and A. Vairo, Phys. Lett. B **470**, 215 (1999) [arXiv:hep-ph/9910238].
- [37] M. B. Voloshin, Sov. J. Nucl. Phys. **36**, 143 (1982) [Yad. Fiz. **36**, 247 (1982)].
- [38] S. Eidelman *et al.* [Particle Data Group Collaboration], Phys. Lett. B **592**, 1 (2004).
- [39] B. A. Kniehl, A. A. Penin, A. Pineda, V. A. Smirnov and M. Steinhauser, Phys. Rev. Lett. **92**, 242001 (2004) [arXiv:hep-ph/0312086].
- [40] M. Artuso *et al.* [CLEO Collaboration], Phys. Rev. Lett. **94**, 032001 (2005) [hep-ex/0411068].
- [41] X. G. i. Tormo and J. Soto, arXiv:hep-ph/0511167.
- [42] N. Brambilla, Y. Sumino and A. Vairo, Phys. Lett. B **513**, 381 (2001) [arXiv:hep-ph/0101305].
- [43] N. Brambilla and A. Vairo, Phys. Rev. D **71**, 034020 (2005) [arXiv:hep-ph/0411156].
- [44] A. A. Penin, V. A. Smirnov and M. Steinhauser, Nucl. Phys. B **716**, 303 (2005) [arXiv:hep-ph/0501042].
- [45] E. E. Salpeter and H. A. Bethe, Phys. Rev. **84**, 1232 (1951).